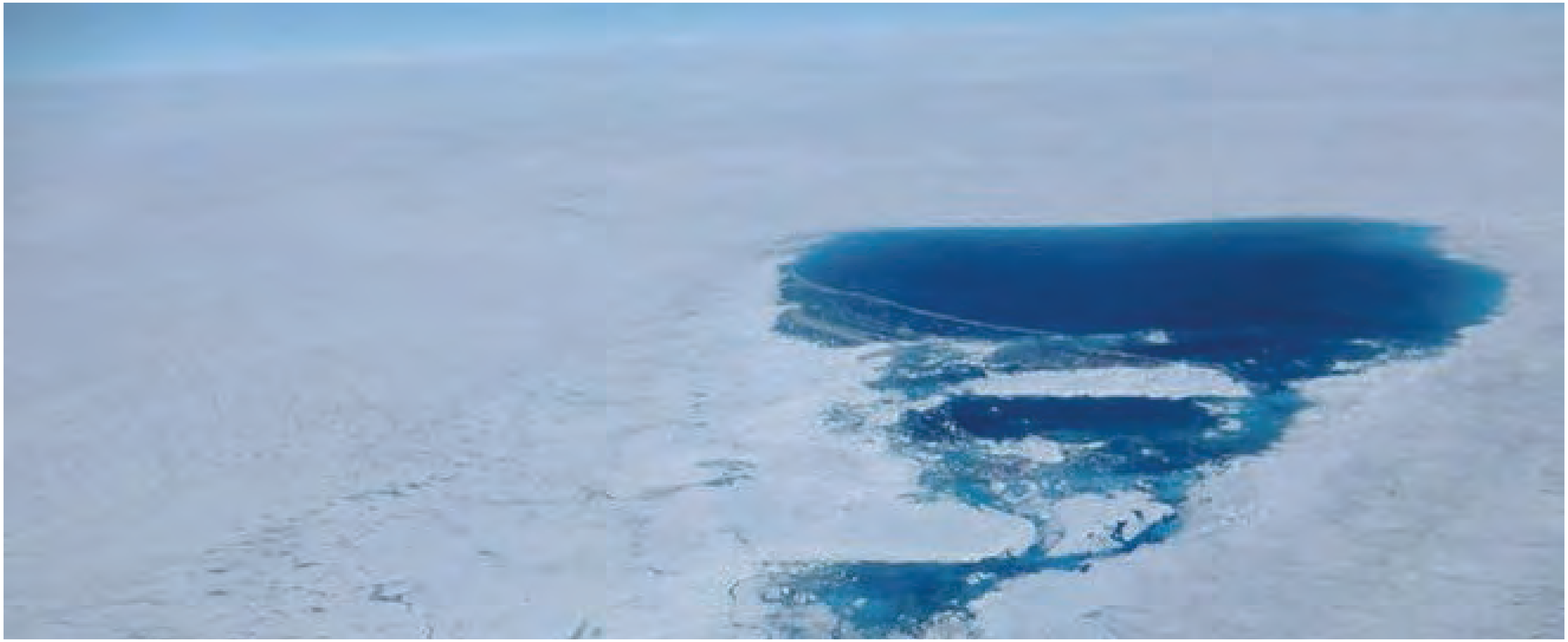

M. Tedesco – Columbia University and NASA GISS

ICE SHEET
SNOW AND MELTING FROM EO

Topics covered by others

- These topics will not be covered for snow over ice sheets because already covered by others during the course. Some of the techniques presented in the following might have already be covered during those classes.

- **Ice sheet and ice shelf altimetry**
- **Altimetry mass balance**
- **Ice sheet mass balance and GRACE**
- **Snow on land and sea ice snow**

OUTLINE

WHAT ?

- Melting
- Accumulation
- Albedo
- Grain size and impurities

OUTLINE

WHAT ?

- Melting
- Accumulation
- Albedo
- Grain size and impurities

HOW ?

- Active and passive microwave
- Optical and thermal remote sensing
- Lidar and radar applications
- GRACE

METHODS AND TOOLS:
ACTIVE AND PASSIVE MICROWAVE REMOTE SENSING

Passive Microwave Radiometry

- Microwave region: 1-200 GHz (0.15-30cm)
- Uses the same principles as thermal remote sensing
- Multi-frequency/multi-polarization sensing
- Weak energy source so needs large IFOV and wide bands

Passive Microwave Radiometry

- Microwave radiometers can measure the emitted spectral radiance received (L_λ)
- This is called the brightness temperature and is linearly related to the kinetic temperature of the surface
- The Rayleigh-Jeans approximation provides a simple linear relationship between measured spectral radiance temperature and emissivity

Brightness Temperature

Brightness temperature is the temperature a **black body** in thermal equilibrium with its surroundings would have to be to duplicate the observed intensity of a grey body object at a frequency *f.*

Brightness temperature can be related to kinetic temperature through emissivity

$$T_b = \varepsilon T_{kin}$$

Thus, passive microwave brightness temperatures can be used to monitor temperature as well as properties related to emissivity

Dielectric Constant/Emissivity of ice

Real part of permittivity of ice is relatively constant (3.15) mostly a function of temperature, with T expressed in [K]*:

$$\mathrm{Re}(\varepsilon_{ice}) = \frac{3.099T - 992.65}{T - 318.896}$$

Imaginary part of permittivity of ice depends on both frequency and temperature:

$$\mathrm{Im}(\varepsilon_{ice}) = \frac{A(T)}{f} + B(T)f$$

f is the frequency in GHz and A(T) and B(T) are temperature-dependent parameters.

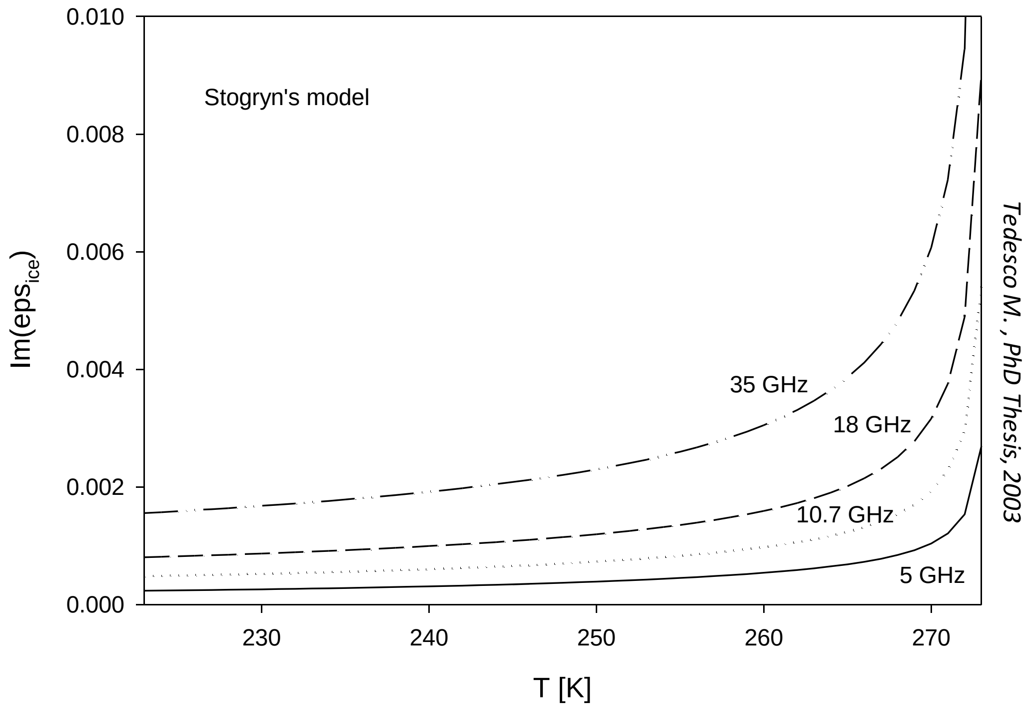

*Imaginary part of ice permittivity as a function of temperature for different frequencies (5 GHz, 10.7 GHz, 18 GHz and 35 GHz) for Stogryn's model**

*) A. Stogryn, "*A study of the microwave brightness temperature of snow from the point of view of strong fluctuation theory*", IEEE Trans. On Geo. And Rem. Sens., Vol. GE-24, No. 2, March 1986, pp 220-231

Dielectric Constant/Emissivity of ice

The loss factor ε'' of ice as a function of frequency. The solid curves display the model proposed by Hufford. Measured data: open diamonds, Westphal , closed circles Wegmüller, crosses, Lamb, open triangles, Lamb and Turney, open circles, Cumming, closed aquares, Mätzler, dashed curve Mishima, open squares, isolated measurements.

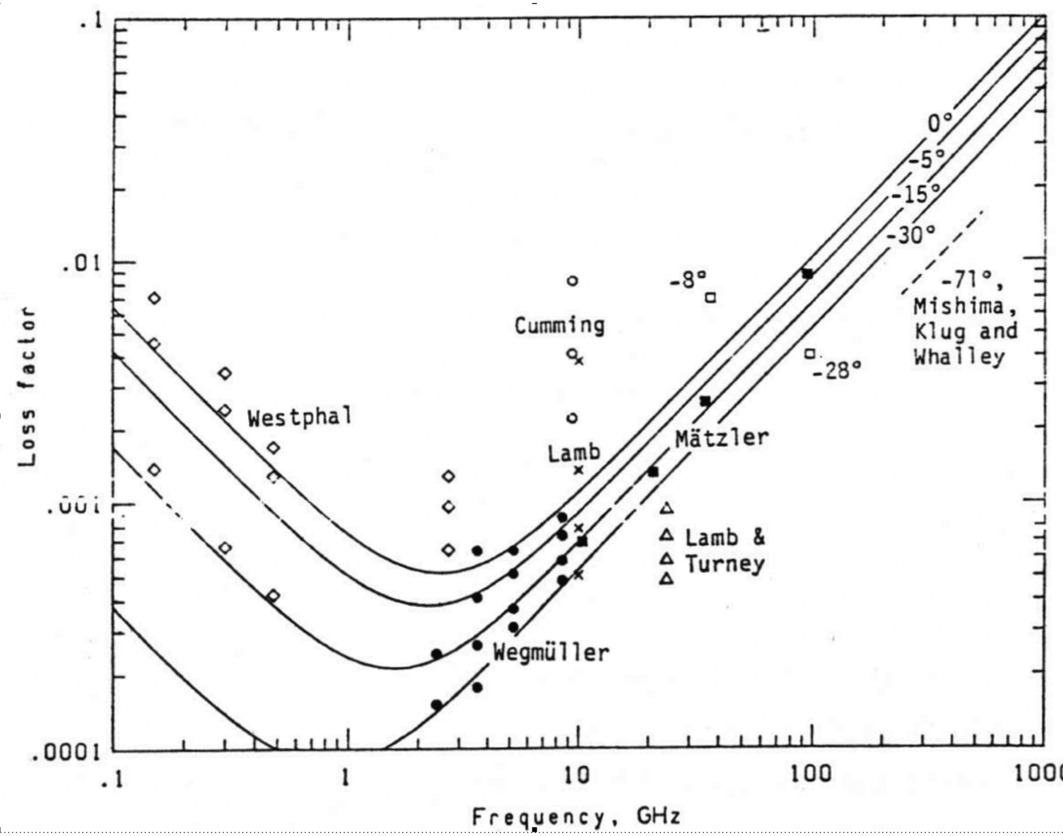

Adapted from Tedesco M. , PhD Thesis, 2003

Dielectric Constant and density

- Dry snow can be seen under an electromagnetic point of view as a mixture of ice and air. Its permittivity depends, therefore, on the permittivities of the single constituent materials and on their fractional volume.
- The real part of dry snow permittivity can be considered constant with frequency and temperature and it strongly depends on the fractional volume

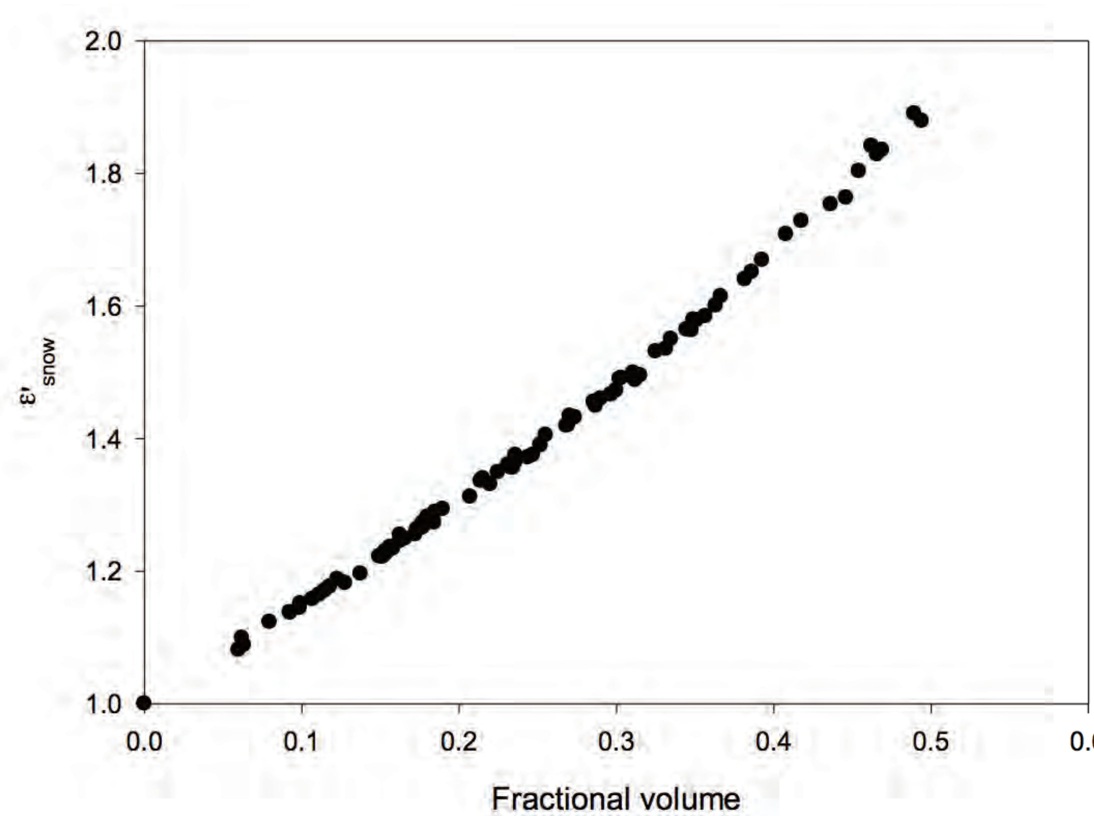

Tedesco M. , PhD Thesis, 2003

Dielectric Constant and density

Empirical relation	Remarks
$\varepsilon' = (1+0.851\rho)^2$	freq≥ 10 MHz
$\varepsilon' = (1+0.508\rho)^3$	freq = 9.375 GHz
$\varepsilon' = 1+1.582/(1-0.365\rho)$	freq = 1 GHz, $\rho \leq 0.45$
$\varepsilon' = 1+ 2.22\rho + 0.41\rho^2$	freq = 3.48 MHz
$\varepsilon' = 1+2\rho$	$4 \leq$ freq ≤ 12 GHz
$\varepsilon' = 1+1.9\rho$ $\varepsilon' = 0.51+2.88\rho$	$3 \leq$ freq ≤ 18 GHz , $\rho \leq 0.5$ $\rho \geq 0.45$
$\varepsilon' = 1+1.92\rho+0.44\rho^2$	$0.01 \leq$ freq ≤ 1 GHz, $\rho \leq 0.65$
$\varepsilon' = 1+1.7\rho+0.7\rho^2$	freq = 1 GHz

Tedesco M. , PhD Thesis, 2003

Dielectric Constant/Emissivity of **DRY** snow

- Sihvola proposes a mixing formula, generalizing the existing mixing formulas for granular media. In the case of ellipsoids isotropically oriented in the vacuum we have

$$\varepsilon = 1 + \frac{f(\varepsilon_s - 1)\sum_{i=1}^{3} \frac{\varepsilon_a}{\varepsilon_a + A_i(\varepsilon_s - 1)}}{3 - f(\varepsilon_s - 1)\sum_{i=1}^{3} \frac{A_i}{\varepsilon_a + A_i(\varepsilon_s - 1)}}$$

where A_i is the depolarisation factor for the i^{th} principal axis and ε_a is the so called apparent permittivity

$$\varepsilon_a = 1 + a(\varepsilon - 1)$$

Sihvola, 1999

Dielectric Constant/Emissivity of **DRY** snow

$$\varepsilon_a = 1 + a(\varepsilon - 1)$$

The formula is able to reproduce measured data with a very good accuracy (standard deviation 0.0064) when the depolarisation factor A ($A = A_1 = A_2$ and $A_3 = 1 - 2A$) is given by:

$$A = \begin{cases} 0.1 + 0.5f \ldots 0 < f < 0.33 \\ 0.18 + 3.24(f - 0.49)^2 \ldots 0.33 \le f < 0.71 \\ 1/3 \ldots f > 0.71 \end{cases}$$

And a= (1-A)

Sihvola, 1999

Dielectric Constant/Emissivity of wet snow

- Wet snow can be seen a mixture of **ice, air and water** which can appear as free or bounded.
- Under a dielectric point of view, wet snow is more difficult than dry snow. One reason for this is that dielectric contrasts are very large in the mixture but at the same time the amount of liquid water is low.
- As a consequence, small changes in the distribution and small-scale structure of the water phase can cause large deviations on the wet snow permittivity.

$$\varepsilon = \varepsilon_{ds} + \Delta\varepsilon$$

- where the first term is the permittivity of the dry snow and the second term takes into account of the effects of the presence of liquid water

Dielectric Constant/Emissivity of wet snow

$$\varepsilon = \varepsilon_{ds} + \Delta\varepsilon$$

The second term can be expressed as a combination of the wetness, with coefficients to be fitted from experimental data.

Empirical relation	Remarks
$\Delta\varepsilon = 0.206 * Wv + 0.0046 Wv^2$	0.01≤freq≤1 GHz
$\Delta\varepsilon = 0.02 * Wv + (0.06 - 3.1 * 10^{-4}(freq-4)^2) Wv^{1.5}$	4≤freq≤12 GHz
$\Delta\varepsilon = 0.089 Wv + 0.0072 Wv^2$	freq = 1 GHz
$\varepsilon'' = 0.073 * (\varepsilon')^{1/2} Wv/freq$	4≤freq≤12 GHz
$\varepsilon'' = 0.009 * Wv + 0.0007 Wv^2$	Freq = 1 GHz
$\varepsilon'' = c(freq) * Wv^{1.5}$	

Tedesco M., PhD Thesis, 2003

Example of melting snow micro-structure

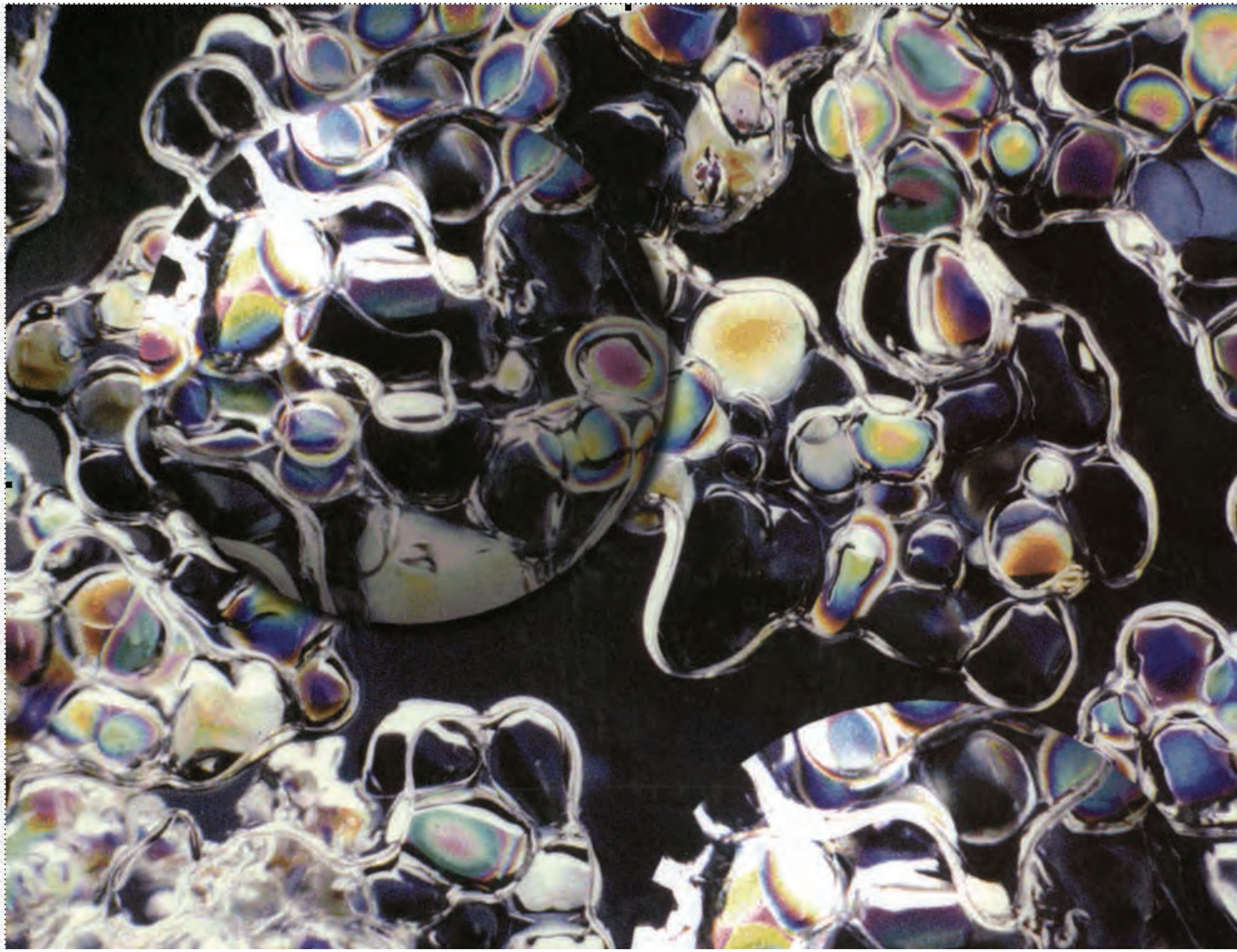

Dielectric Constant/Emissivity of wet snow (spherical particles covered by water film)

- The effective permittivity of a spherical particle with permittivity ε_1 and radius *r1* covered by a film of a material with permittivity ε_2 and radius *r2* can be computed as

$$\frac{\varepsilon - \varepsilon_0}{\varepsilon + 2\varepsilon_0} = \frac{(\varepsilon_2 - \varepsilon_0)(\varepsilon_1 + \varepsilon_2) + S(\varepsilon_1 - \varepsilon_2)(\varepsilon_0 + 2\varepsilon_2)}{(\varepsilon_2 + 2\varepsilon_0)(\varepsilon_1 + 2\varepsilon_2) + 2S(\varepsilon_2 - \varepsilon_0)(\varepsilon_1 - \varepsilon_2)}$$

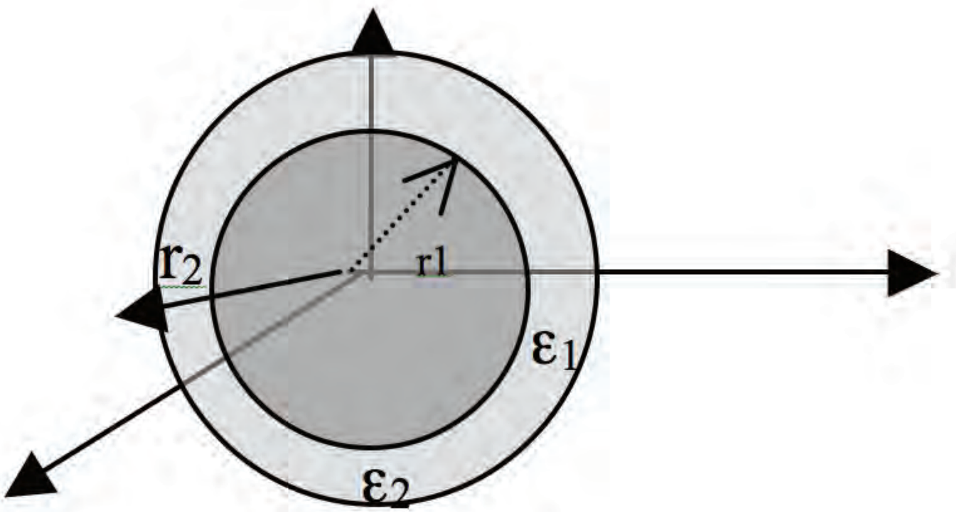

Wher $S = a_1/a_2$ where a_1 and a_2 are, respectively, the inner and the outer radii of the sphere

Sihvola, 1999

Dielectric Constant/Emissivity of wet snow

- From an electromagnetic point of view snow can be seen as a mix of air, ice and liquid water (in the case of wet snow)
- Several mixing formulas have been proposed in the literature

Fraction (by volume)

$$\varepsilon^b = \varepsilon_h^b (1 - f) + \varepsilon_s^b f$$

Host medium

Scatterers permittivity

Since the dry snow permittivity is of the order of while the water inclusions have a permittivity that can be 40 times larger, even when the liquid water content is on the order of only 1% by volume, the spectral behavior of wet snow is dominated by the dispersion behavior of water

$$\varepsilon = \left(\varepsilon_{ds}^{1/3}(1 - Wv) + \varepsilon_{watere}^{1/3} Wv\right)^3$$

Sihvola, 1999

In case of wet snow and b = 3

Examples of wet snow permittivity

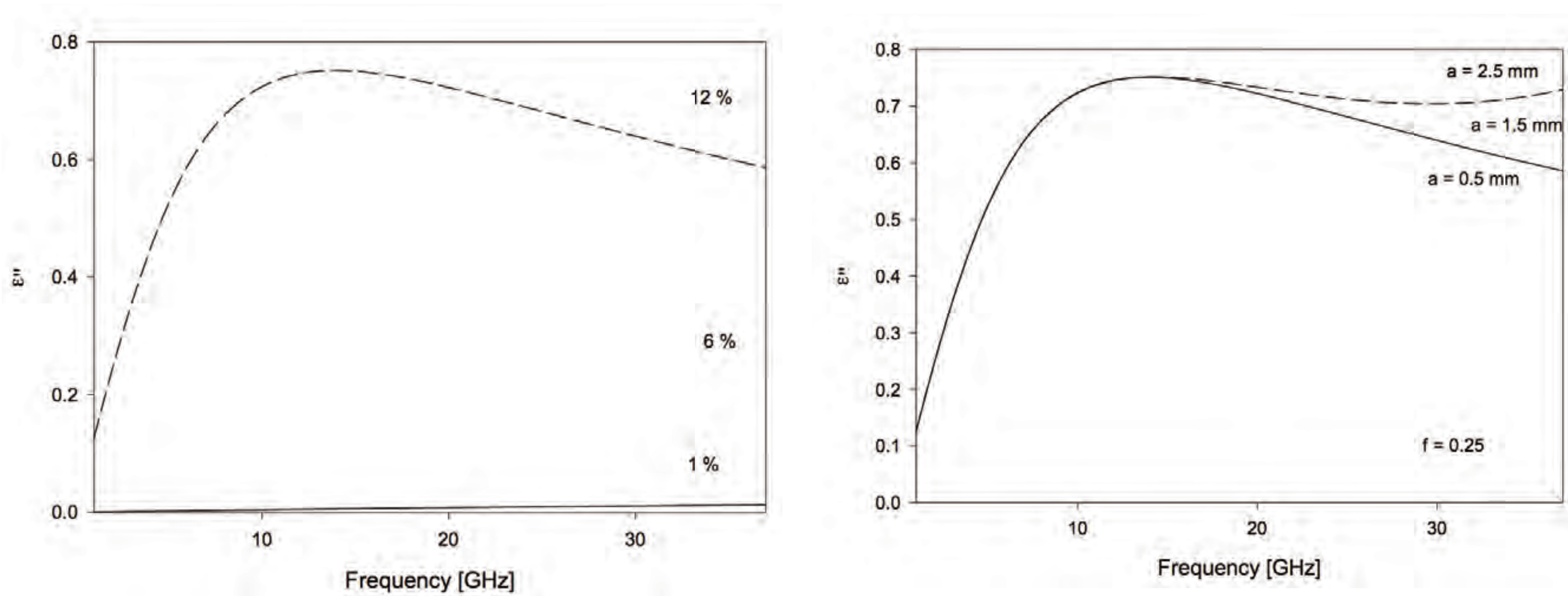

Tedesco M. , PhD Thesis, 2003

Behavior of imaginary part of wet snow permittivity using the DMRT with fractional volume f = 0.25 and different radii or wetness

Examples of wet snow permittivity

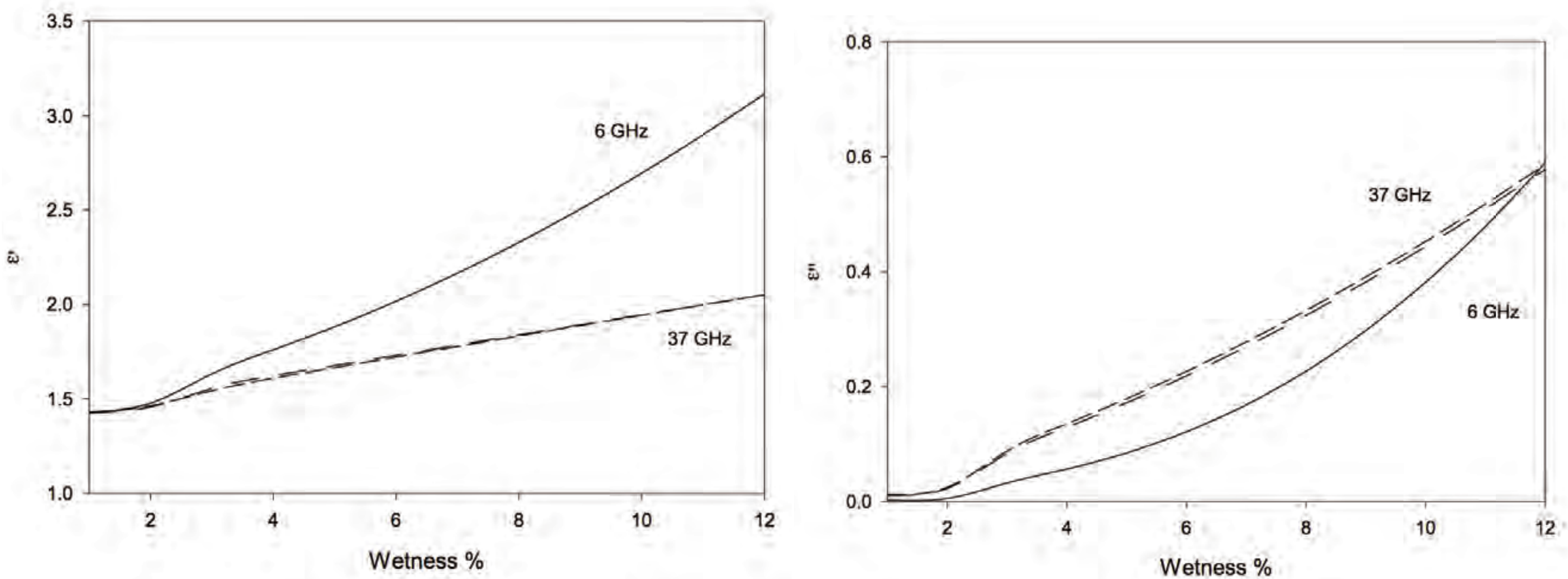

Tedesco M. , PhD Thesis, 2003

Real and imaginary part of the effective permittivity of wet snow as a function of wetness at 6 and 37 GHz for a fixed fractional volume and grain radius (f = 0.25 and a = 0.5 mm)

Passive Microwave Remote Sensing from Space

Advantages

- Penetration through non-precipitating clouds
- Radiance is linearly related to temperature (i.e. the retrieval is nearly linear)
- Highly stable instrument calibration
- Global coverage and wide swath
- Sensitive to sub-surface processes (e.g., allows snow depth , wetness estimates)

Disadvantages

- Larger field of views (10-50 km) compared to VIS/IR sensors
- Variable emissivity over land
- Polar orbiting satellites provide discontinuous temporal coverage at low latitudes (e.g., need to create weekly composites)
- Strong sensitivity to wetness (saturates → doesn't allow

Spaceborne Microwave Radiometers

- Advanced Microwave Sounding Unit (AMSU) 1978-present
- Scanning Multichannel Microwave Radiometer (SMMR) 1981 - 1987
- Special Sensor Microwave/Imager (SSM/I - SSMIS) 1987-present
- Advanced Microwave Scanning Radiometer for EOS (AMSR-E) 2002-2011
- Advanced Microwave Scanning Radiometer/2 (AMSR2) 2012 – to present
- TRMM-TMI
- WindSAT
- SMOS
- AQUARIUS
- GPM

Parameter	SMMR (Nimbus-7)	SSM/I (DMSP-F08,F10,F11,F13)	AMSR-E (Aqua)	AMSR (ADEOS-II)
Time Period	1978 to 1987	1987 to Present	Beginning 2001	Beginning 2002
Frequencies (GHz)	6.6, 10.7, 18, 21, 37	19.3, 22.3, 36.5, 85.5	6.9, 10.7, 18.7, 23.8, 36.5, 89.0	6.9, 10.65, 18.7, 23.8, 36.5, 89.0, 50.3, 52.8
Sample Footprint Sizes (km):	148 x 95 (6.6 GHz) 27 x 18 (37 GHz)	37 x 28 (37 GHz) 15 x 13 (85.5 GHz)	74 x 43 (6.9 GHz) 14 x 8 (36.5 GHz) 6 x 4 (89.0 GHz)	74 x 43 (6.9 GHz) 14 x 8 (36.5 GHz) 6 x 4 (89.0 GHz)

Special Sensor Microwave/Imager (SSM/I - SSMIS) 1987-present

Channel	Center Frequency (GHz)	3-db Width (MHz)	Frequency Stability (MHz)	Polarization	NEΔT (K)[I]	Sampling Interval (km)[II]	Channel Application
1	50.3	380	10	V	034	37.5	LAS
2	52.8	389	10	V	0.32	37.5	LAS
3	53.596	380	10	V	0.33	37.5	LAS
4	54.4	383	10	V	0.33	37.5	LAS
5	55.5	391	10	V	0.34	37.5	LAS
6	57.29	330	10	RCP[IV]	0.41	37.5	LAS
7	59.4	239	10	RCP	0.40	37.5	LAS
8	150	1642(2)[III]	200	H	0.89	12.5	IMA
9	183.31 ± 6.6	1526(2)	200	H	0.97	12.5	IMA
10	183.31 ± 3	1019(2)	200	H	0.67	12.5	IMA
11	183.31 ± 1	513(2)	200	H	0.81	12.5	IMA
12	19.35	355	75	H	0.33	25	ENV
13	19.35	357	75	V	0.31	25	ENV
14	22.235	401	75	V	0.43	25	ENV
15	37	1616	75	H	0.25	25	ENV
16	37	1545	75	V	0.20	25	ENV
17	91.655	1418(2)	100	V	0.33	12.5	IMA
18	91.655	1411(2)	100	H	0.32	12.5	IMA
19	63.283248 ± 0.285271	1.35(2)	0.08	RCP	2.7	75	UAS
20	60.792668 ± 0.357892	1.35(2)	0.08	RCP	2.7	75	UAS
21	60.792668 ± 0.357892 ± 0.002	1.3(4)	0.08	RCP	1.9	75	UAS
22	60.792668 ± 0.357892 ± 0.0055	2.6(4)	0.12	RCP	1.3	75	UAS
23	60.792668 ± 0.357892 ± 0.016	7.35(4)	0.34	RCP	0.8	75	UAS
24	60.792668 ± 0.357892 ± 0.050	26.5(4)	0.84	RCP	0.9	37.5	LAS

Advanced Microwave Scanning Radiometer for EOS (AMSR-E) 2002-2010

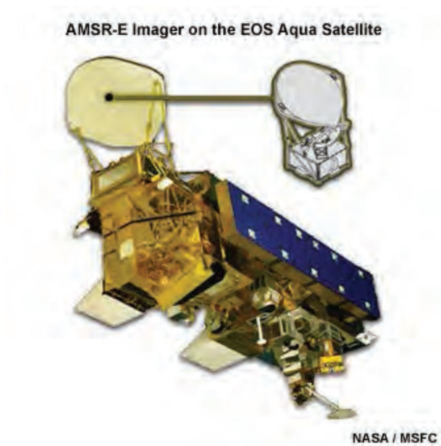

Polarization	Horizontal and vertical					
Incidence angle	55°					
Cross-polarization	Less than -20 dB					
Swath	1445 km					
Dynamic Range (K)	2.7 to 340					
Precision	1 K (1σ)					
Quantifying Bit Number	12-bit	10-bit				
Center Frequency (GHz)	6.925	10.65	18.7	23.8	36.5	89.0
Bandwidth (MHz)	350	100	200	400	1000	3000
Sensitivity (K)	0.3	0.6				1.1
Mean Spatial Resolution (km)	56	38	21	24	12	5.4
IFOV (km)	74 x 43	51 x 30	27 x 16	31 x 18	14 x 8	6 x 4
Sampling Interval (km)	10 x 10					5 x 5
Integration Time (msec)	2.6					1.3
Main Beam Efficiency (%)	95.3	95.0	96.3	96.4	95.3	96.0
Beamwidth (degrees)	2.2	1.4	0.8	0.9	0.4	0.18

Swath/coverage for different PMW sensors

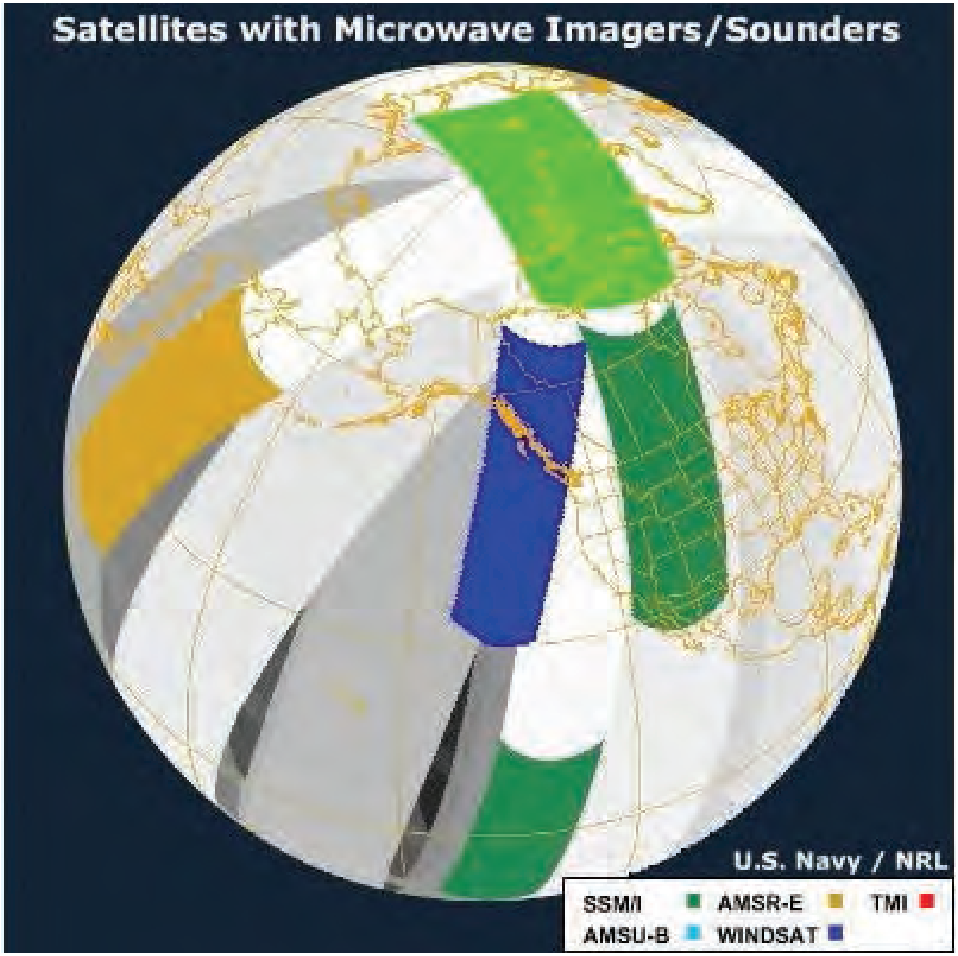

Microwave emissivity
Dry vs. wet snow

The presence of dry snow on soil attenuates the microwave radiation naturally emitted by the soil, therefore reducing the measured brightness temperature with respect to the bare soil case (left). Higher brightness temperature values are recorded in the case of the presence of wet snow (right), which absorbs the radiation from the bottom layer and emits a signal stronger than that of the dry snow covering soil or ice.

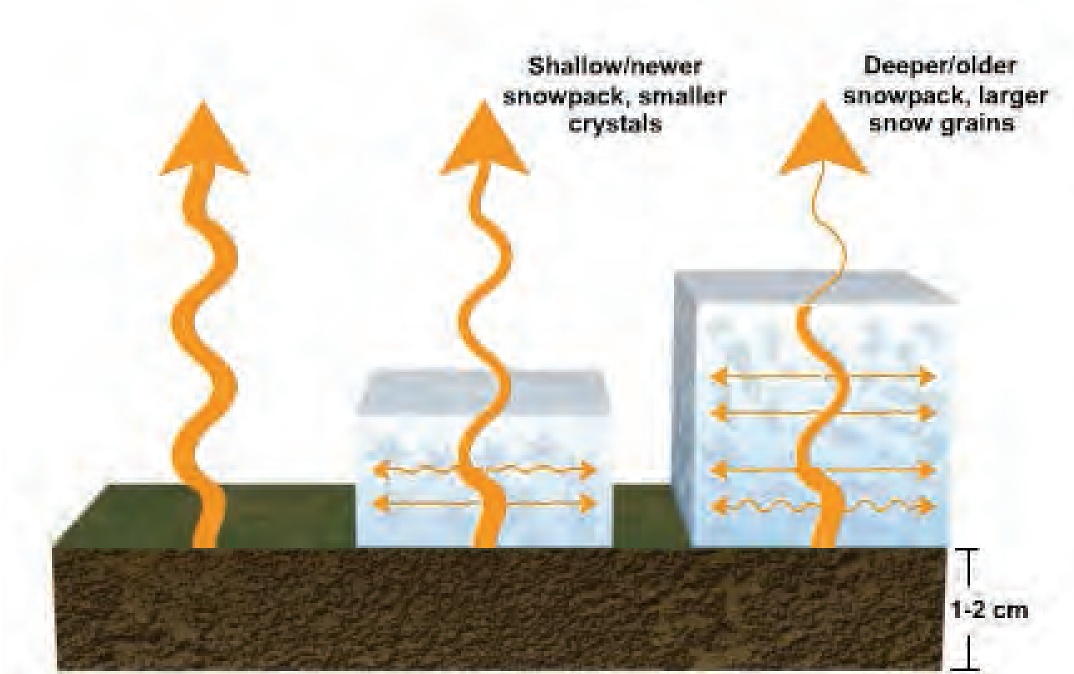

Example of brightness temperature of dry vs. wet snow

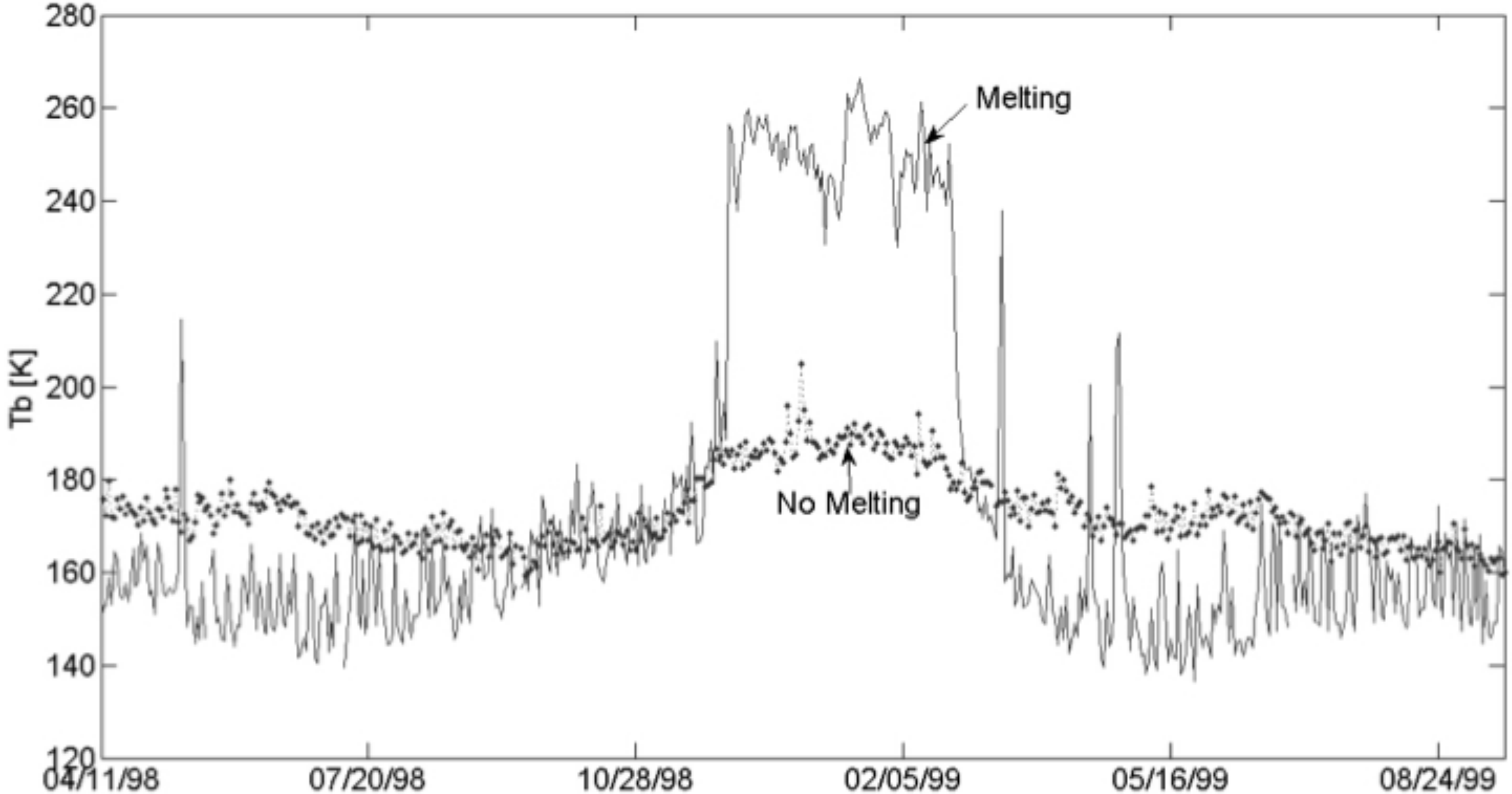

Tedesco M. , 2007

Active microwave remote sensing

- A directed beam of microwave pulses are transmitted from an antenna
- The energy interacts with the terrain and is scattered
- The backscattered microwave energy is measured by the antenna
- Radar determines the direction and distance of the target from the instrument as well as the backscattering properties of the target

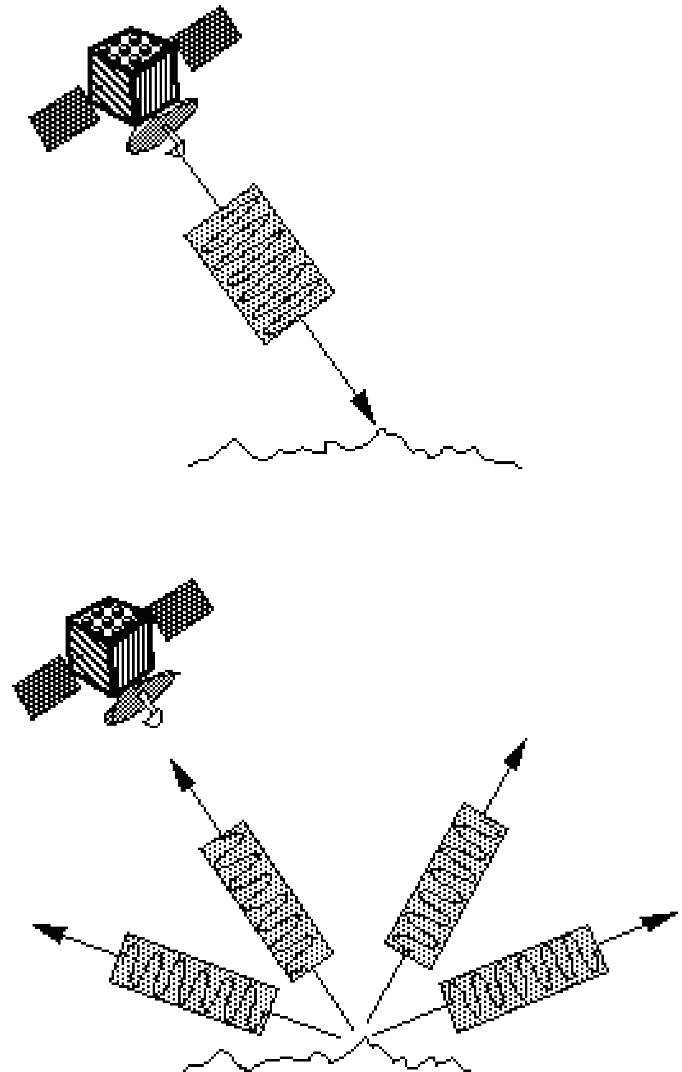

Radar Backscatter

$$\boxed{\text{Power received}} = \boxed{\text{Power per unit area at target}} \times \boxed{\text{Effective scattering area of the target}} \times \boxed{\text{Spreading loss of reradiated signal}} \times \boxed{\text{Effective receiving area of antenna}}$$

Radar Backscatter Coefficient

The efficiency the terrain to reflect the radar pulse is termed the "*radar cross-section*", ?

The radar cross-section per unit area, (A) is called the "*radar backscatter coefficient*" (?°) and is computed as :

$$\sigma^o = \frac{\sigma}{A}$$

The *radar backscatter coefficient* determines the percentage of electro-magnetic energy reflected back to the radar from within a radar pixel

This is similar to the reflectance in optical remote sensing

Spaceborne Microwave active sensors

- TRMM – PR
- RADARSAT
- ASCAT
- CloudSat
- Jason 1-2-3
- ENVISAT
- ERS
- Sentinel-1
- Cryosat-2

Backscattering of dry vs. wet snow

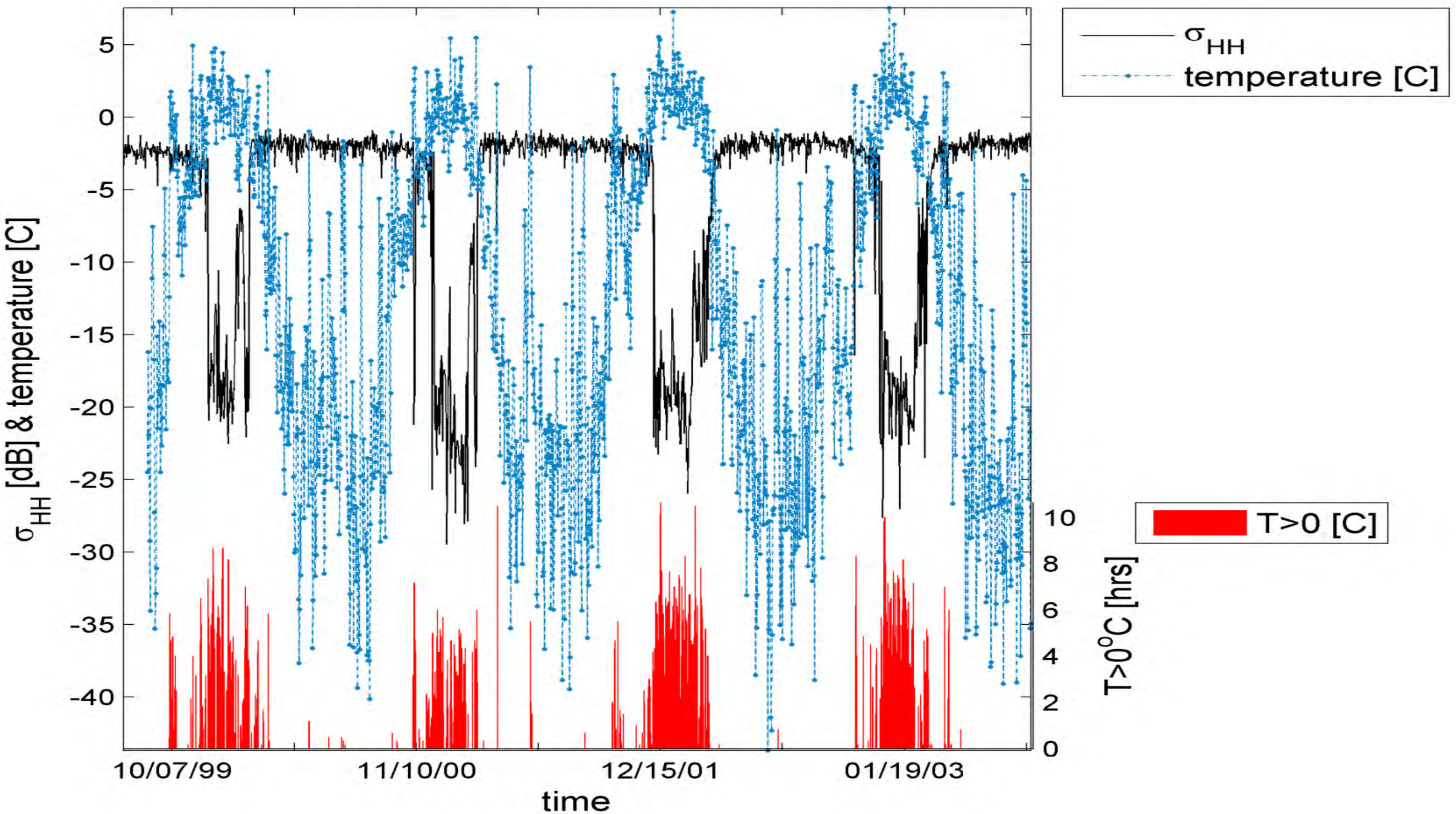

EXAMPLE OF TB AND BACKSCATTERING OF SNOW COVERED TERRAIN

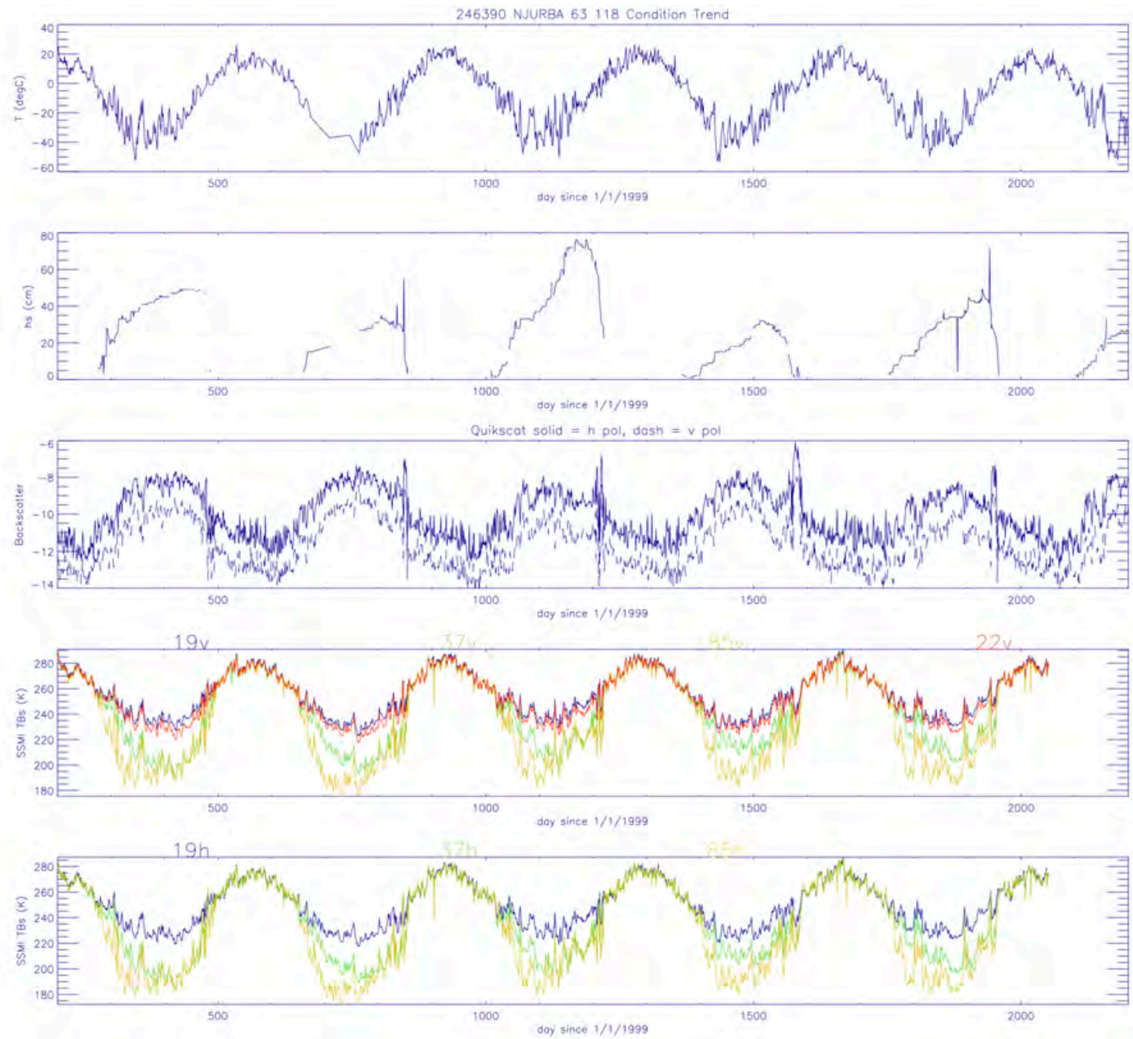

Tedesco et al., 2007

APPLICATIONS:
SNOW MELT

Melt detection techniques

Melting is detected when Tbs (or backscattering), or a combination of multiple frequencies and polarizations, exceeds (is below) a computed threshold value

- Diurnal Amplitude Variations (Passive MW)
- Inversion of electromagnetic models (Passive and active MW)
- XPGR (Passive MW)
- Wavelet (Passive and active MW)
- Fixed threshold (Active and Passive MW)
- Surface temperature (Thermal)

Melt detection techniques: XPGR

$$XPGR = \frac{T_b(19H) - T_b(37V)}{T_b(19H) + T_b(37V)}$$

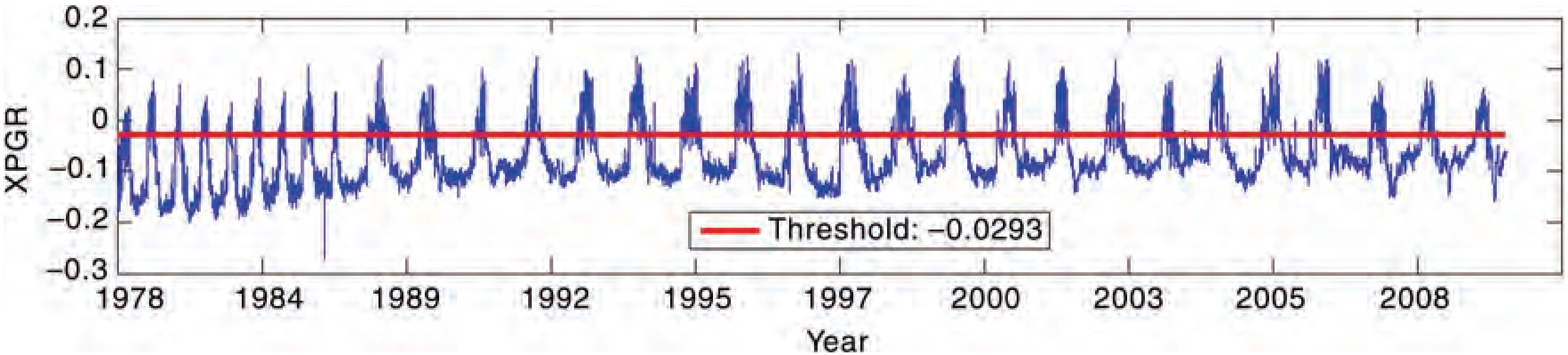

Melting is detected when XPGR exceeds a set threshold value (Abdalati and Steffen, 1997)

Melt detection techniques: inversion of EM models

Annual Tbs are assumed to have a bimodal distribution and the threshold value above which snow is assumed to be melting is computed as the Tb value whose probability to belong to the melting distribution is maximized

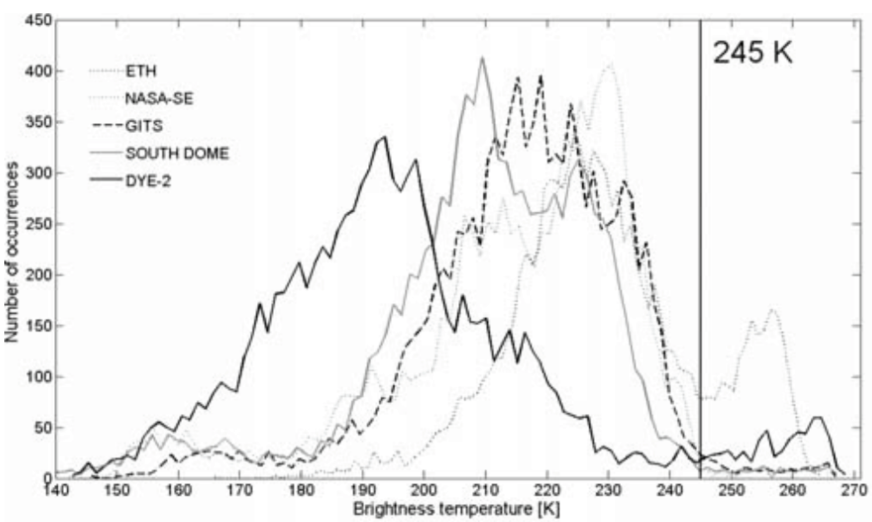

Tedesco , 2007

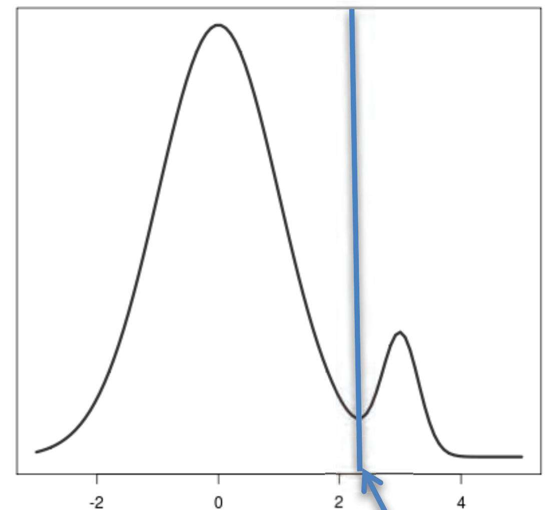

Spatial and temporal dynamic coefficients

Melting over Greenland from PMW

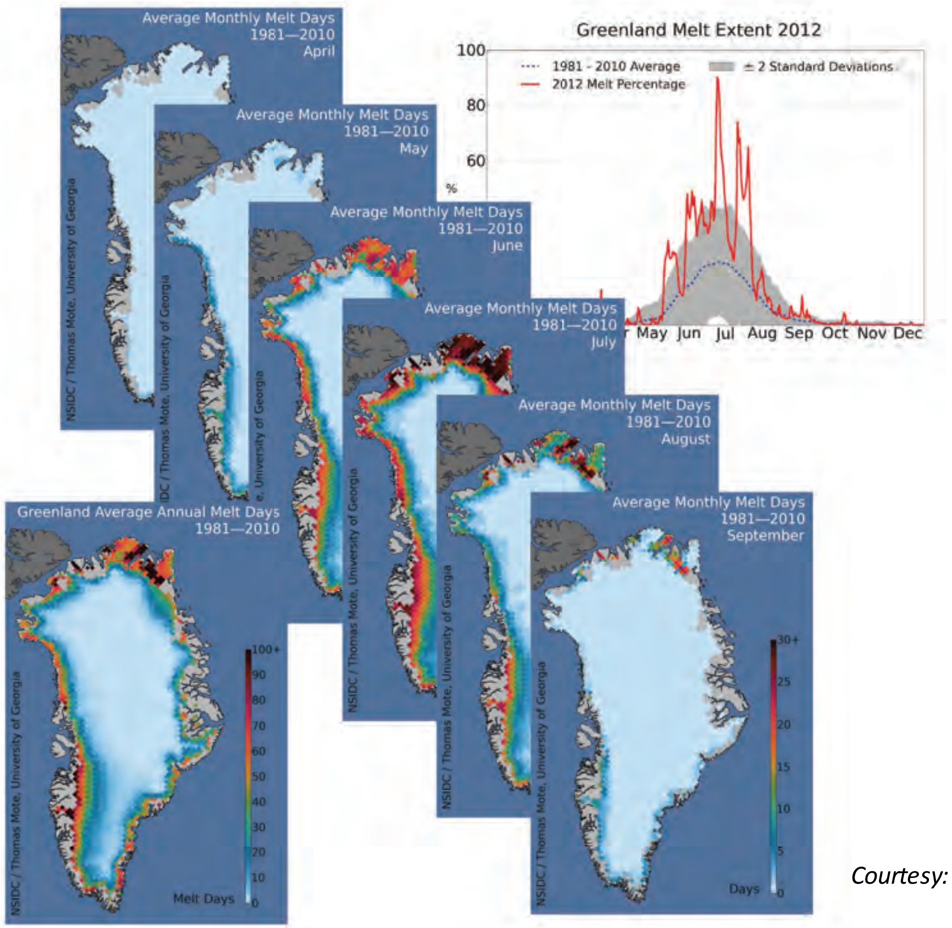

Courtesy: NSIDC

Melting over Greenland from PMW

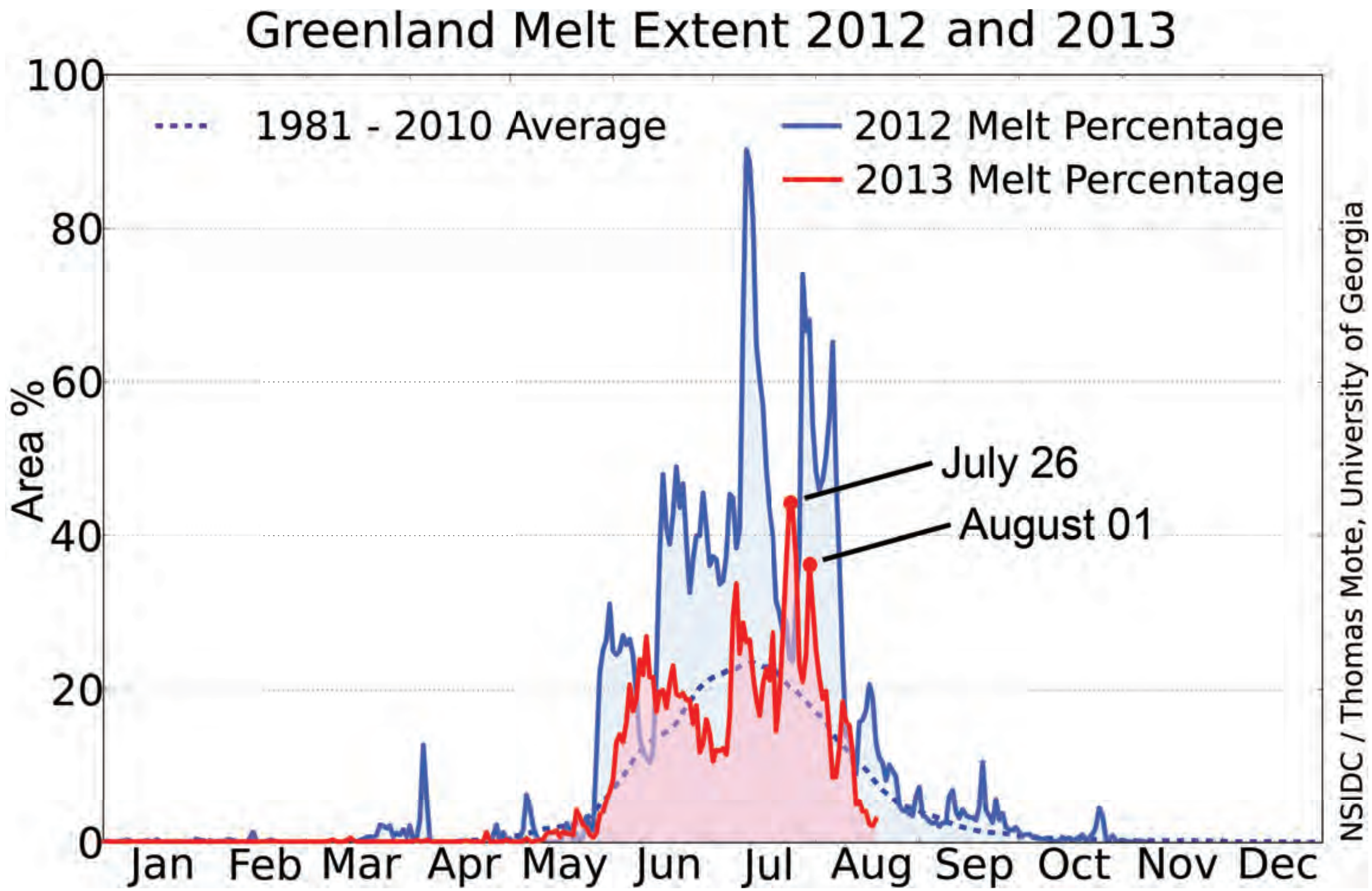

Melting over Greenland from PMW

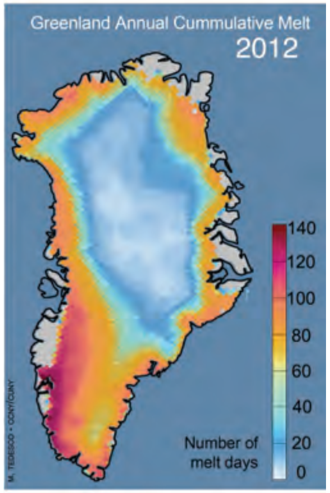

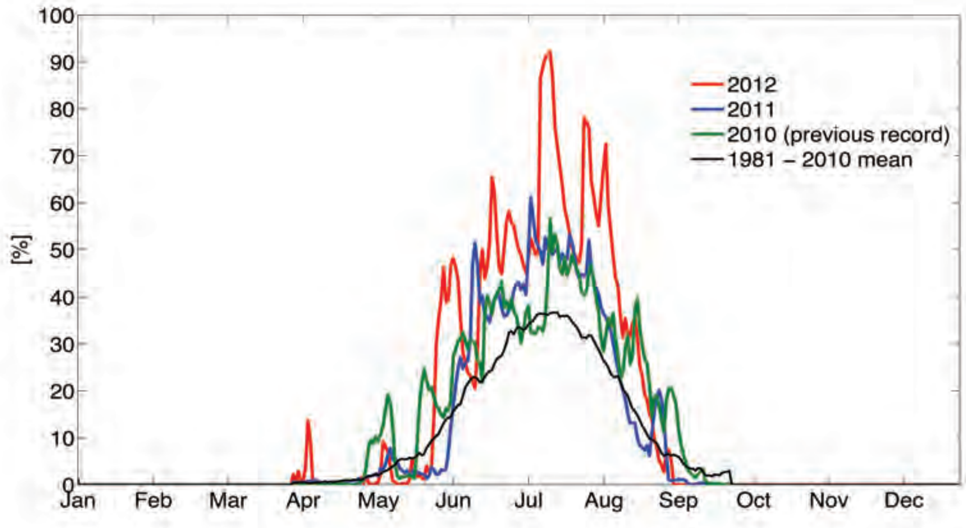

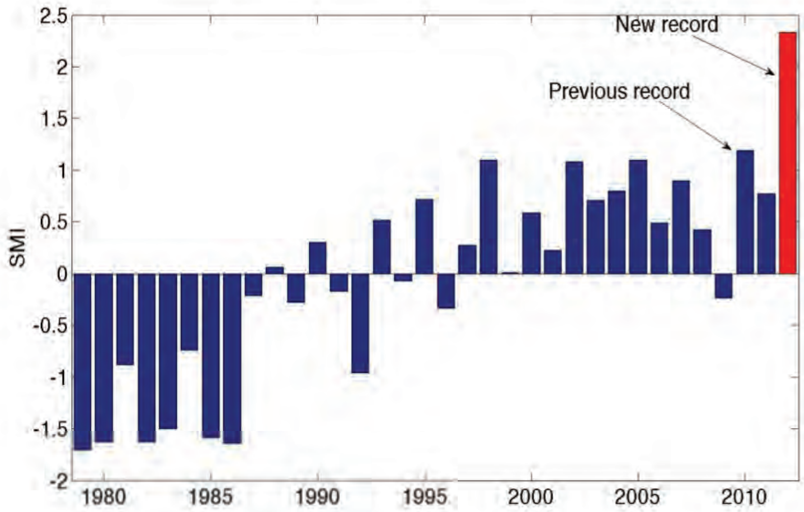

- Number of melting days and % of Greenland undergoing melting from passive microwave

M. Tedesco

Melting from thermal (MODIS) data

Maps of annual maximum melt extent constructed from MODIS IST data of the Greenland ice sheet for the study period (March 2000 through August 2012). The non-ice covered land surrounding the ice sheet is shown in green. The boundaries of the six major drainage basins of the Greenland ice sheet (after Zwally et al., 2005) are superimposed on the maps (Data and image courtesy: NASA).

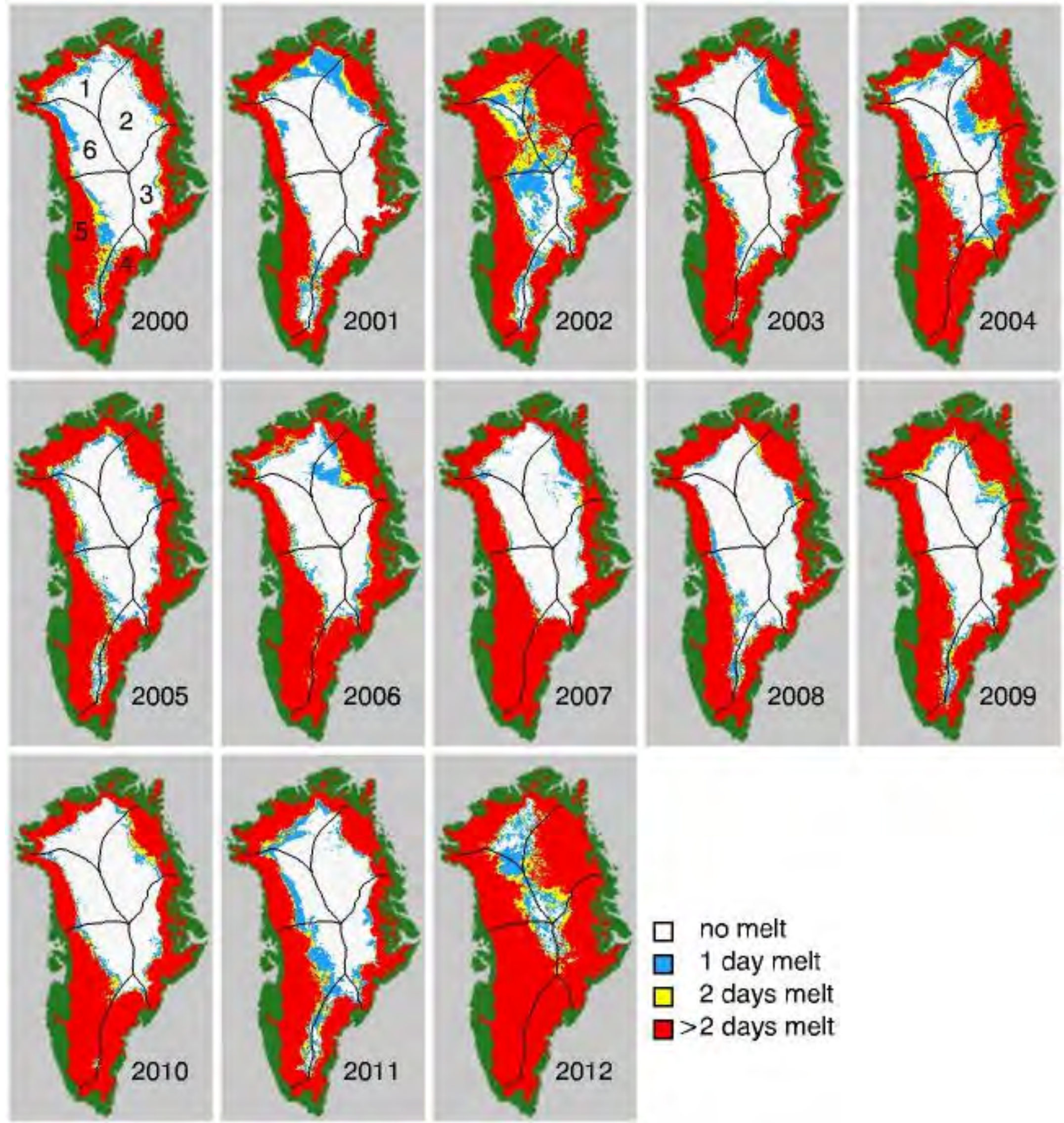

Multi-sensor melt detection

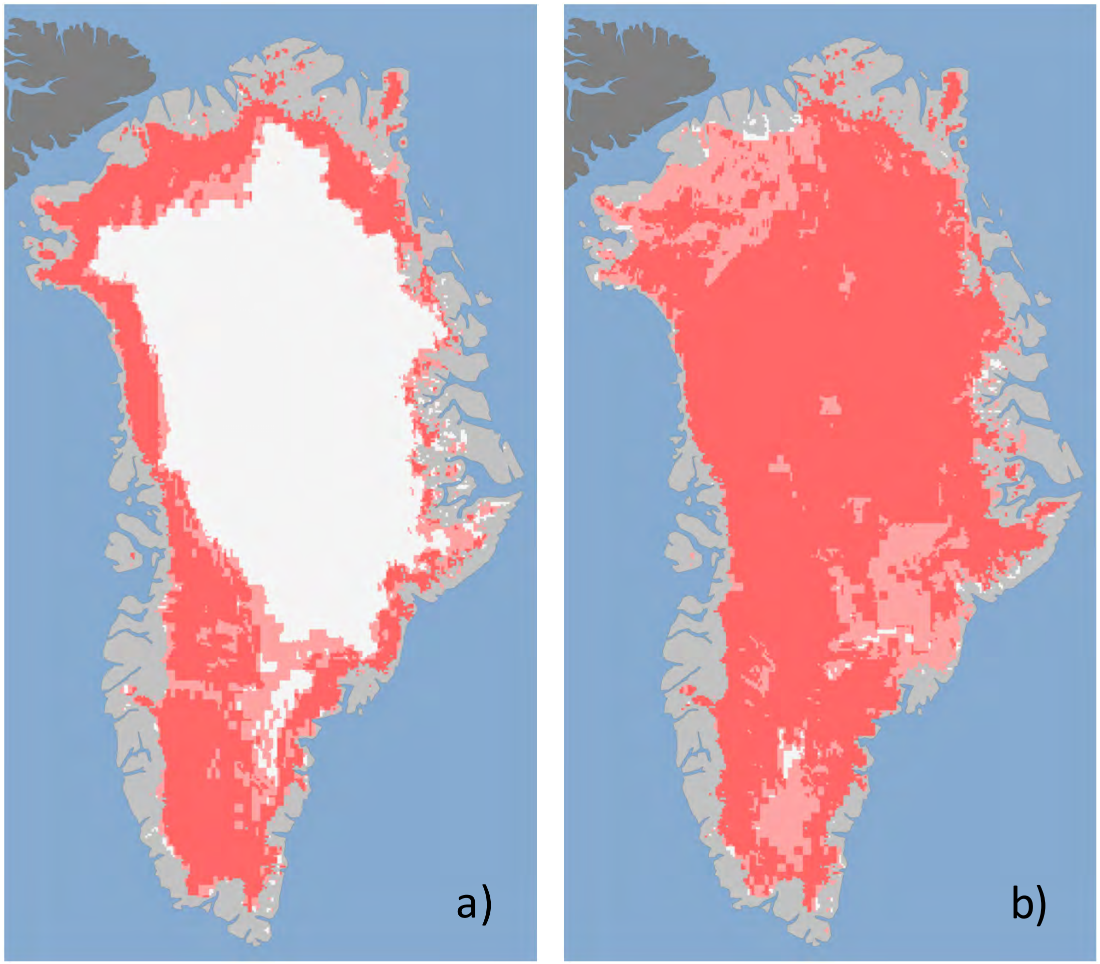

Extent of surface melt over the Greenland ice sheet on a) July 8 and b) July 12. Multiple sensors (PMW, AMW, MODIS) were used. The areas classified as “probable melt” (light pink) correspond to those sites where at least one satellite detected surface melting. The areas classified as “melt” (dark pink) correspond to sites where two or three satellites detected surface melting.

Credit : NASA

Melt extent and duration over the Antarctica ice sheet (from active MW)

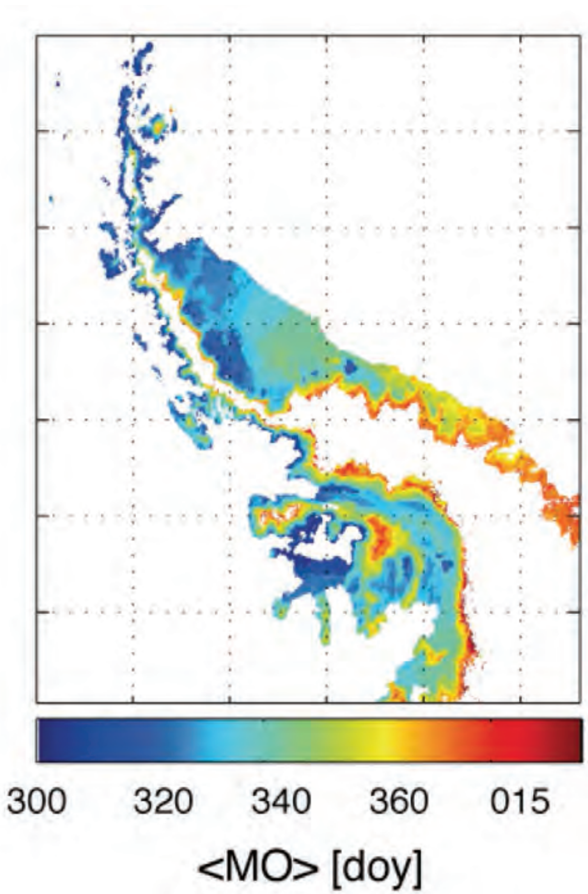

Steiner and Tedesco, 2015

Accumulation from passive MW observations

Arthern et al. (2006) map of Antarctic accumulation in kg/m^2/a (or mm of water equivalent per year) derived from passive microwave AMSR-E data at 6.9 GHz and ice surface temperatures from the Advanced Very High Resolution Radiometer (AVHRR). Map created with data available from the British Antarctic Survey (http://www.antarctica.ac.uk//bas_research/data/online_resources/snow_accumulation/)

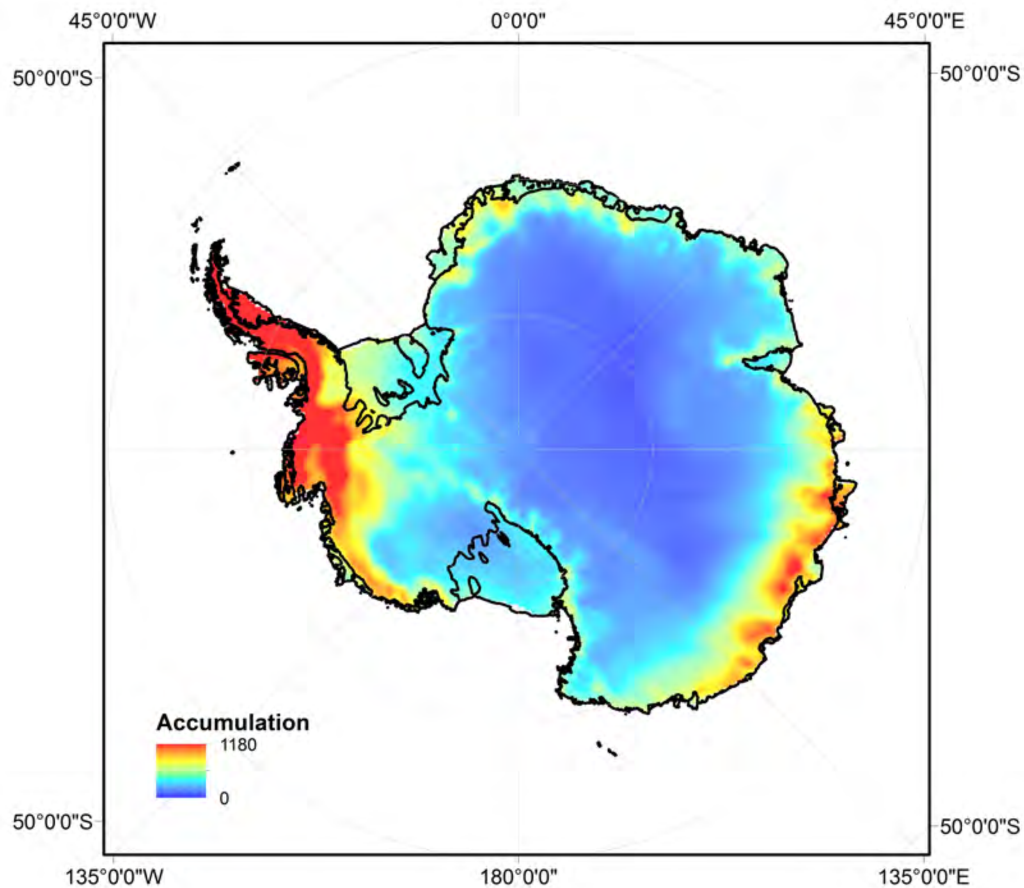

Blowing Snow: Satellite Sources

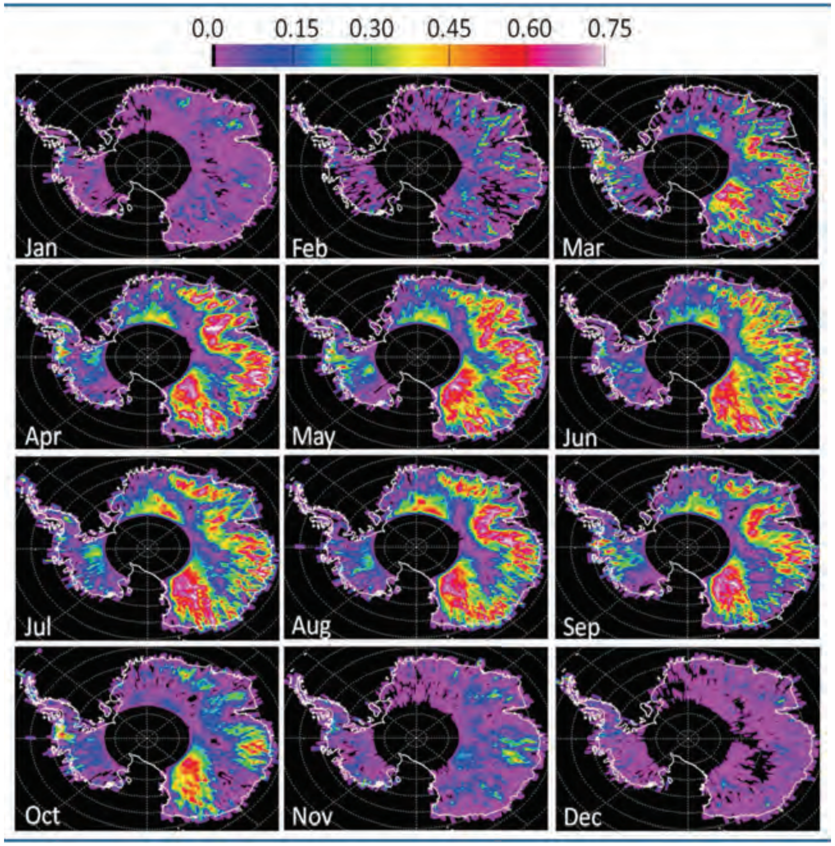

Palm et al, 2011

The blowing snow frequency (fraction) and spatial distribution over Antarctica for each month of 2009 as determined from analysis of CALIPSO data.

METHODS AND TOOLS:
OPTICAL REMOTE SENSING

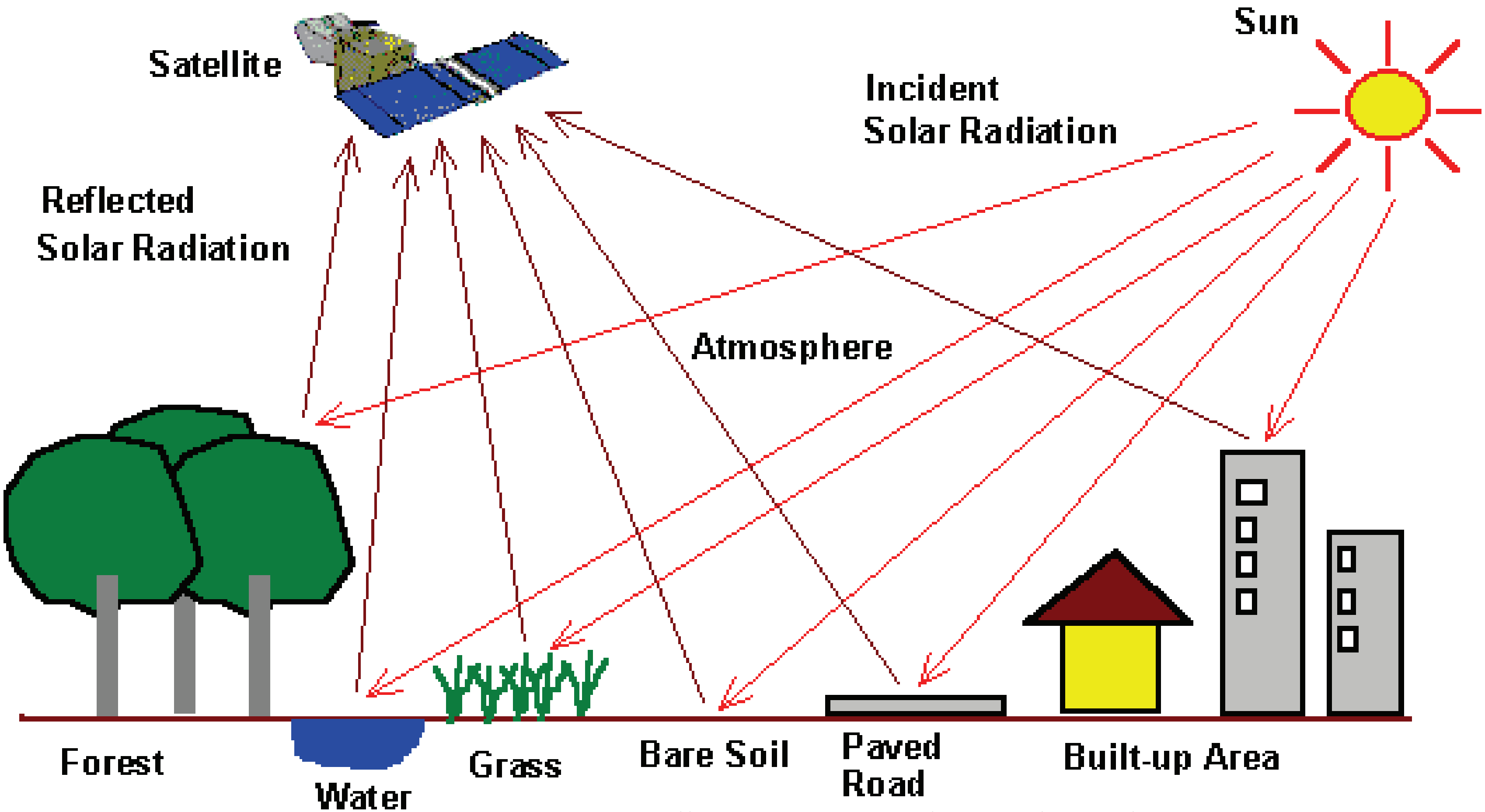

http://www.crisp.nus.edu.sg/~research/tutorial/optical.htm

Visible/NIR vs MW

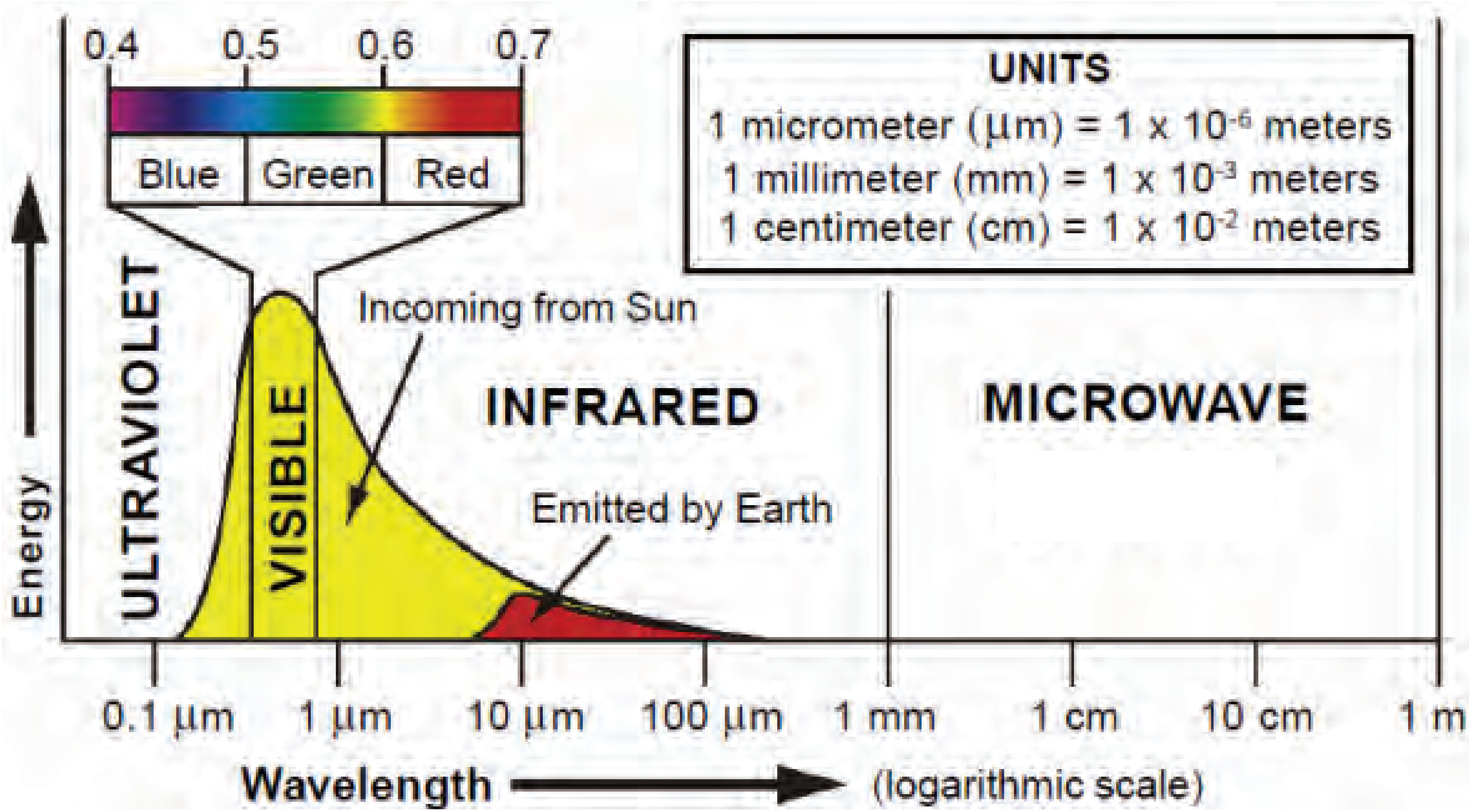

http://remote-sensing.net/concepts.html

Optical/NIR spaceborne sensors

- MODIS / MERIS / ASTER
- AVHRR
- LANDSAT
- WorldView / SPOT / Ikonos
- Hyperion
- Sentinel – 2

MODIS – Moderate Resolution Imaging Spectroradiometer

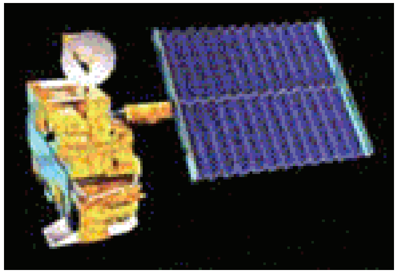

Orbit:	705 km, 10:30 a.m. descending node (Terra) or 1:30 p.m. ascending node (Aqua), sun-synchronous, near-polar, circular
Scan Rate:	20.3 rpm, cross track
Swath Dimensions:	2330 km (cross track) by 10 km (along track at nadir)
Telescope:	17.78 cm diam. off-axis, afocal (collimated), with intermediate field stop
Size:	1.0 x 1.6 x 1.0 m
Weight:	228.7 kg
Power:	162.5 W (single orbit average)
Data Rate:	10.6 Mbps (peak daytime); 6.1 Mbps (orbital average)
Quantization:	12 bits
Spatial Resolution:	250 m (bands 1-2) 500 m (bands 3-7) 1000 m (bands 8-36)
Design Life:	6 years

MODIS – Moderate Resolution Imaging Spectroradiometer

Primary Use	Band	Bandwidth[1]	Spectral Radiance[2]	Required SNR[3]
Land/Cloud/Aerosols Boundaries	1	620 - 670	21.8	128
	2	841 - 876	24.7	201
Land/Cloud/Aerosols Properties	3	459 - 479	35.3	243
	4	545 - 565	29.0	228
	5	1230 - 1250	5.4	74
	6	1628 - 1652	7.3	275
	7	2105 - 2155	1.0	110
Ocean Color/ Phytoplankton/ Biogeochemistry	8	405 - 420	44.9	880
	9	438 - 448	41.9	838
	10	483 - 493	32.1	802
	11	526 - 536	27.9	754
	12	546 - 556	21.0	750
	13	662 - 672	9.5	910
	14	673 - 683	8.7	1087
	15	743 - 753	10.2	586
	16	862 - 877	6.2	516
Atmospheric Water Vapor	17	890 - 920	10.0	167
	18	931 - 941	3.6	57
	19	915 - 965	15.0	250

Primary Use	Band	Bandwidth[1]	Spectral Radiance[2]	Required NE[delta]T(K)[4]
Surface/Cloud Temperature	20	3.660 - 3.840	0.45(300K)	0.05
	21	3.929 - 3.989	2.38(335K)	2.00
	22	3.929 - 3.989	0.67(300K)	0.07
	23	4.020 - 4.080	0.79(300K)	0.07
Atmospheric Temperature	24	4.433 - 4.498	0.17(250K)	0.25
	25	4.482 - 4.549	0.59(275K)	0.25
Cirrus Clouds Water Vapor	26	1.360 - 1.390	6.00	150(SNR)
	27	6.535 - 6.895	1.16(240K)	0.25
	28	7.175 - 7.475	2.18(250K)	0.25
Cloud Properties	29	8.400 - 8.700	9.58(300K)	0.05
Ozone	30	9.580 - 9.880	3.69(250K)	0.25
Surface/Cloud Temperature	31	10.780 - 11.280	9.55(300K)	0.05
	32	11.770 - 12.270	8.94(300K)	0.05
Cloud Top Altitude	33	13.185 - 13.485	4.52(260K)	0.25
	34	13.485 - 13.785	3.76(250K)	0.25
	35	13.785 - 14.085	3.11(240K)	0.25
	36	14.085 - 14.385	2.08(220K)	0.35

LANDSAT

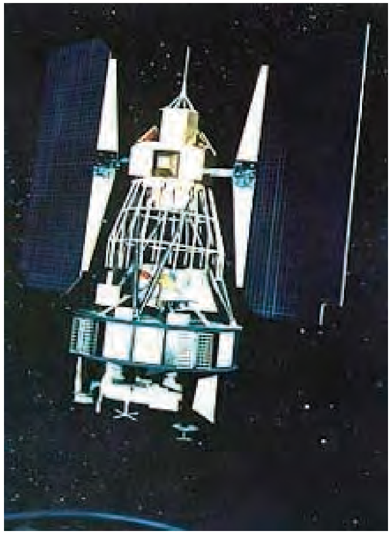

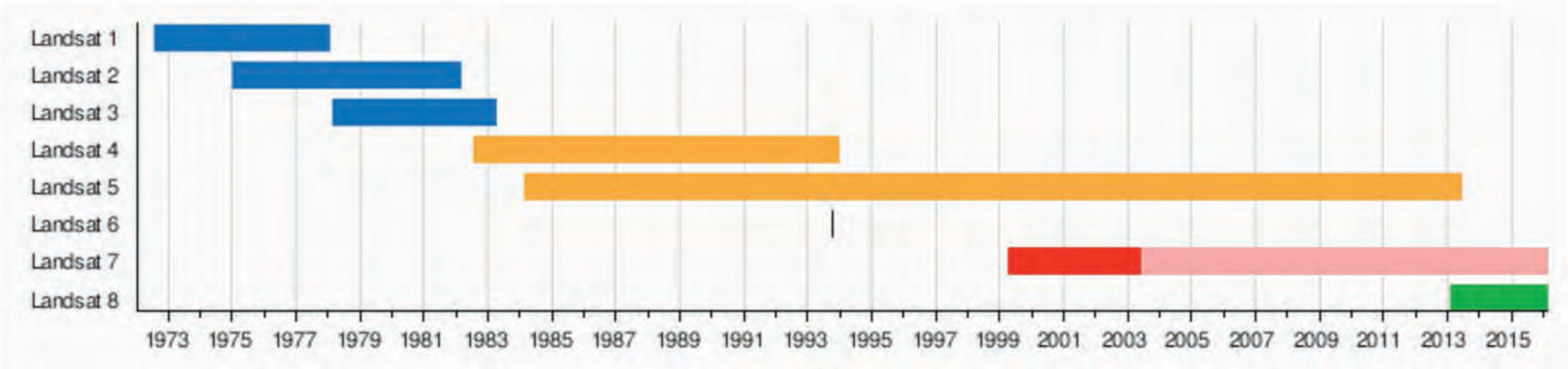

Landsat 1
Landsat 2
Landsat 3
Landsat 4
Landsat 5
Landsat 6
Landsat 7
Landsat 8
1973 1975 1977 1979 1981 1983 1985 1987 1989 1991 1993 1995 1997 1999 2001 2003 2005 2007 2009 2011 2013 2015

LANDSAT-8

Operational Land Imager (OLI)

Spectral Band	Wavelength	Resolution	Solar Irrandiace
Band 1 - Coastal / Aerosol	0.433 – 0.453 μm	30 m	2031 W/(m²μm)
Band 2 - Blue	0.450 – 0.515 μm	30 m	1925 W/(m²μm)
Band 3 - Green	0.525 – 0.600 μm	30 m	1826 W/(m²μm)
Band 4 - Red	0.630 – 0.680 μm	30 m	1574 W/(m²μm)
Band 5 - Near Infrared	0.845 – 0.885 μm	30 m	955 W/(m²μm)
Band 6 - Short Wavelength Infrared	1.560 – 1.660 μm	30 m	242 W/(m²μm)
Band 7 - Short Wavelength Infrared	2.100 – 2.300 μm	30 m	82.5 W/(m²μm)
Band 8 - Panchromatic	0.500 – 0.680 μm	15 m	1739 W/(m²μm)
Band 9 - Cirrus	1.360 – 1.390 μm	30 m	361 W/(m²μm)

Thermal Infrared Sensor

Spectral Band	Wavelength	Resolution
Band 10 - Long Wavelength Infrared	10.30 – 11.30 μm	100 m
Band 11 - Long Wavelength Infrared	11.50 – 12.50 μm	100 m

Worldview

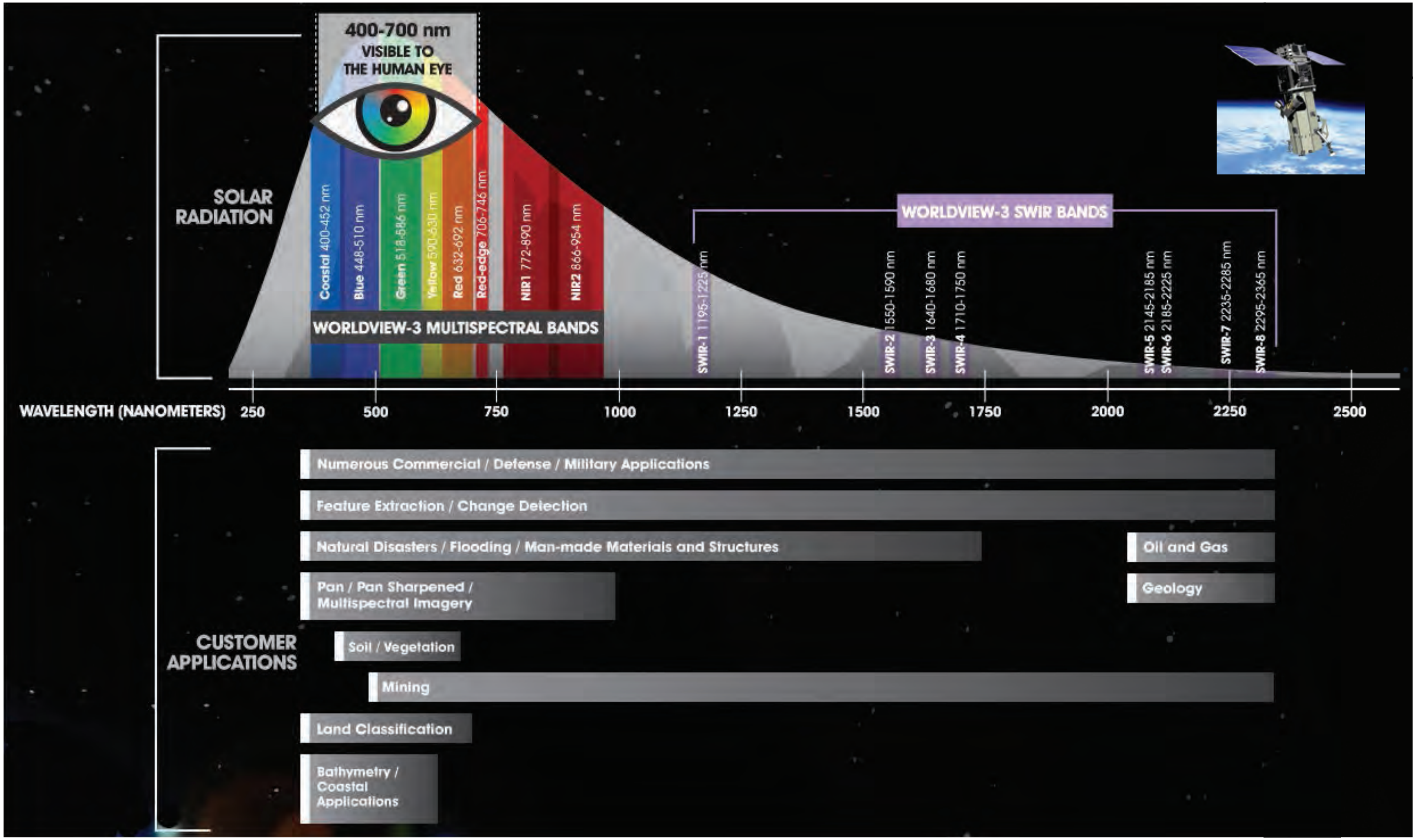
400-700 nm
VISIBLE TO THE HUMAN EYE
SOLAR RADIATION
Coastal 400-452 nm
Blue 448-510 nm
Green 518-586 nm
Yellow 590-630 nm
Red 632-692 nm
Red-edge 706-746 nm
NIR1 772-890 nm
NIR2 866-954 nm
WORLDVIEW-3 MULTISPECTRAL BANDS
WORLDVIEW-3 SWIR BANDS
SWIR-1 1195-1225 nm
SWIR-2 1550-1590 nm
SWIR-3 1640-1680 nm
SWIR-4 1710-1750 nm
SWIR-5 2145-2185 nm
SWIR-6 2185-2225 nm
SWIR-7 2235-2285 nm
SWIR-8 2295-2365 nm
WAVELENGTH (NANOMETERS)
250
500
750
1000
1250
1500
1750
2000
2250
2500
CUSTOMER APPLICATIONS
Numerous Commercial / Defense / Military Applications
Feature Extraction / Change Detection
Natural Disasters / Flooding / Man-made Materials and Structures
Oil and Gas
Pan / Pan Sharpened / Multispectral Imagery
Geology
Soil / Vegetation
Mining
Land Classification
Bathymetry / Coastal Applications

Worldview

	Frequency range observed by band			
Band Name	**QuickBird**	**WorldView-1**	**WorldView-2**	**WorldView-3**
Panchromatic	450-900nm	400-900nm	450-800nm	450-800nm
Coastal Blue			400-450nm	400-450nm
Blue	450-520nm		450-510nm	450-510nm
Green	520-600nm		510-580nm	510-580nm
Yellow			585-625nm	585-625nm
Red	630-690nm		630-690nm	630-690nm
Red Edge			705-745nm	705-745nm
NIR-1	760-900nm		770-895nm	770-895nm
NIR-2			860-1040nm	860-1040nm
SWIR-1				1195-1225nm
SWIR-2				1550-1590nm
SWIR-3				1640-1680nm
SWIR-4				1710-1750nm
SWIR-5				2145-2185nm
SWIR-6				2185-2225nm
SWIR-7				2235-2285nm
SWIR-8				2295-2365nm

Hyperion

The Hyperion provides a high resolution hyperspectral imager capable of resolving **220 spectral bands** (from 0.4 to 2.5 μm) with a **30-meter** resolution. The instrument can image a 7.5 km by 100 km land area per image, and provide detailed spectral mapping across all 220 channels with high radiometric accuracy

Link to table of bands: https://eo1.usgs.gov/sensors/hyperioncoverage

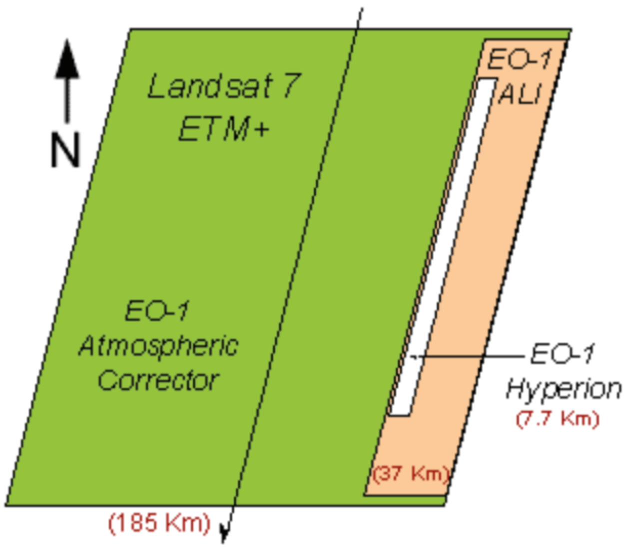

Hyperion vs. ASTER vs. LANDSAT

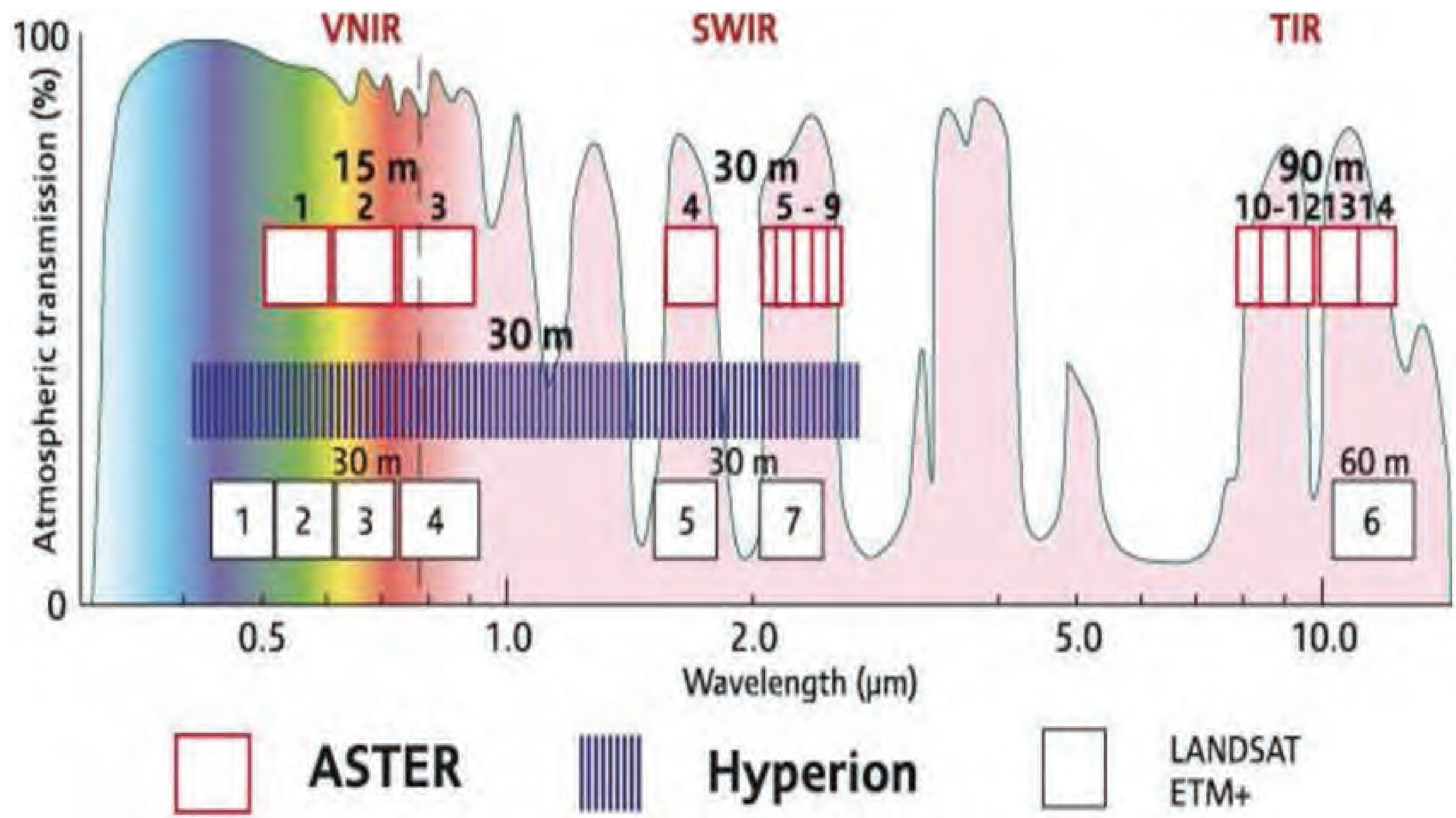

Sentinel - 2

- Launched on June 2015
- Multi-spectral data with 13 bands in the visible, near infrared, and short wave infrared part of the spectrum
- Systematic global coverage of land surfaces from 56° S to 84° N, coastal waters, and all of the Mediterranean Sea
- Revisiting every 5 days under the same viewing angles. At high latitudes, Sentinel-2 swath overlap and some regions will be observed twice or more every 5 days, but with different viewing angles.
- Spatial resolution of 10 m, 20 m and 60 m
- 290 km field of view

Sentinel - 2

Sentinel-2 Bands	Central Wavelength (μm)	Resolution (m)
Band 1 - Coastal aerosol	0.443	60
Band 2 - Blue	0.490	10
Band 3 - Green	0.560	10
Band 4 - Red	0.665	10
Band 5 - Vegetation Red Edge	0.705	20
Band 6 - Vegetation Red Edge	0.740	20
Band 7 - Vegetation Red Edge	0.783	20
Band 8 - NIR	0.842	10
Band 8A - Vegetation Red Edge	0.865	20
Band 9 - Water vapour	0.945	60
Band 10 - SWIR - Cirrus	1.375	60
Band 11 - SWIR	1.610	20
Band 12 - SWIR	2.190	20

Sentinel – 2 vs. LANDSAT

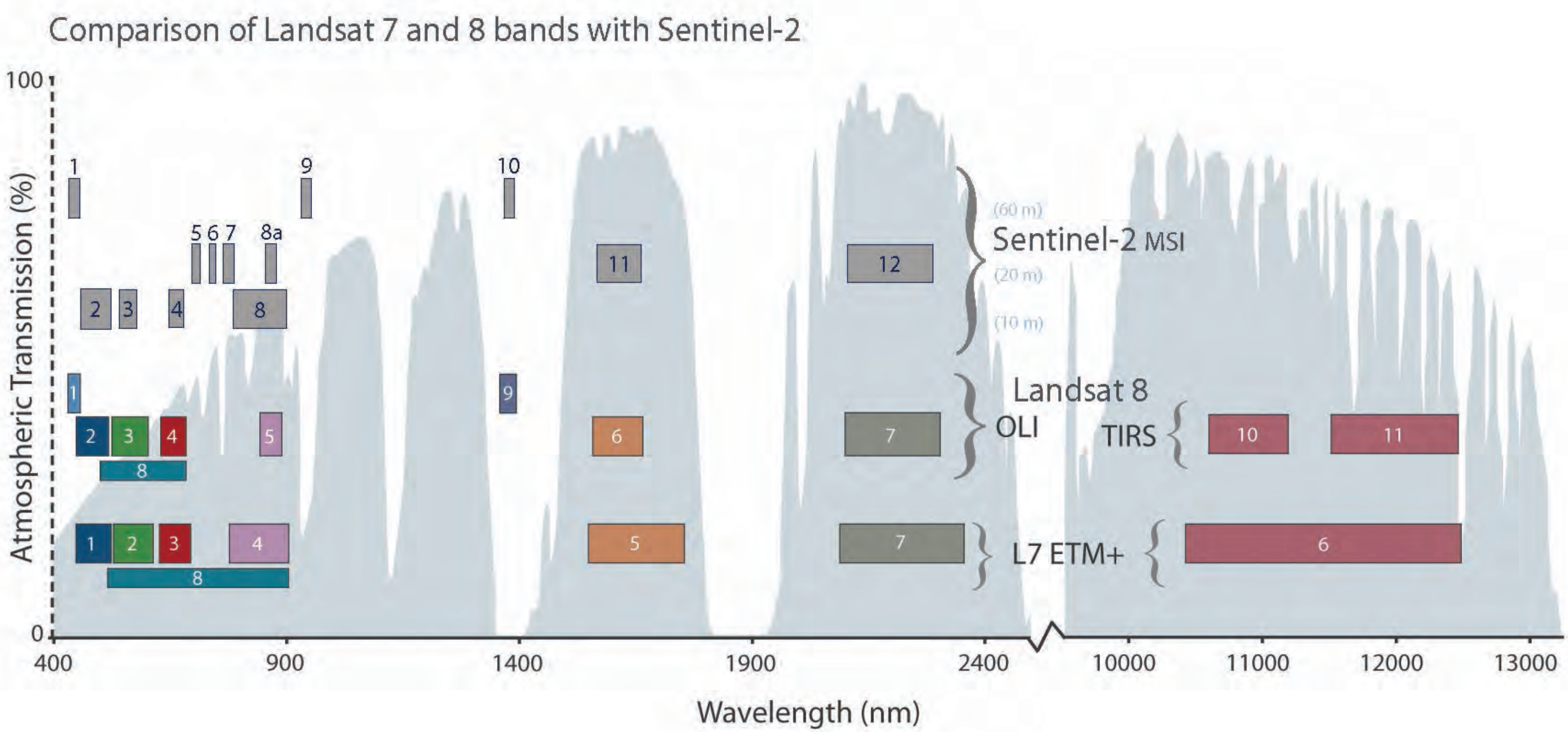

Reflectance spectra

Reflectance spectra of several typical materials encountered in satellite imagery of glacierized terrain, and pass bands of several sensors in the visible and near-infrared (VNIR), and short-wave infrared (SWIR) parts of the spectrum.

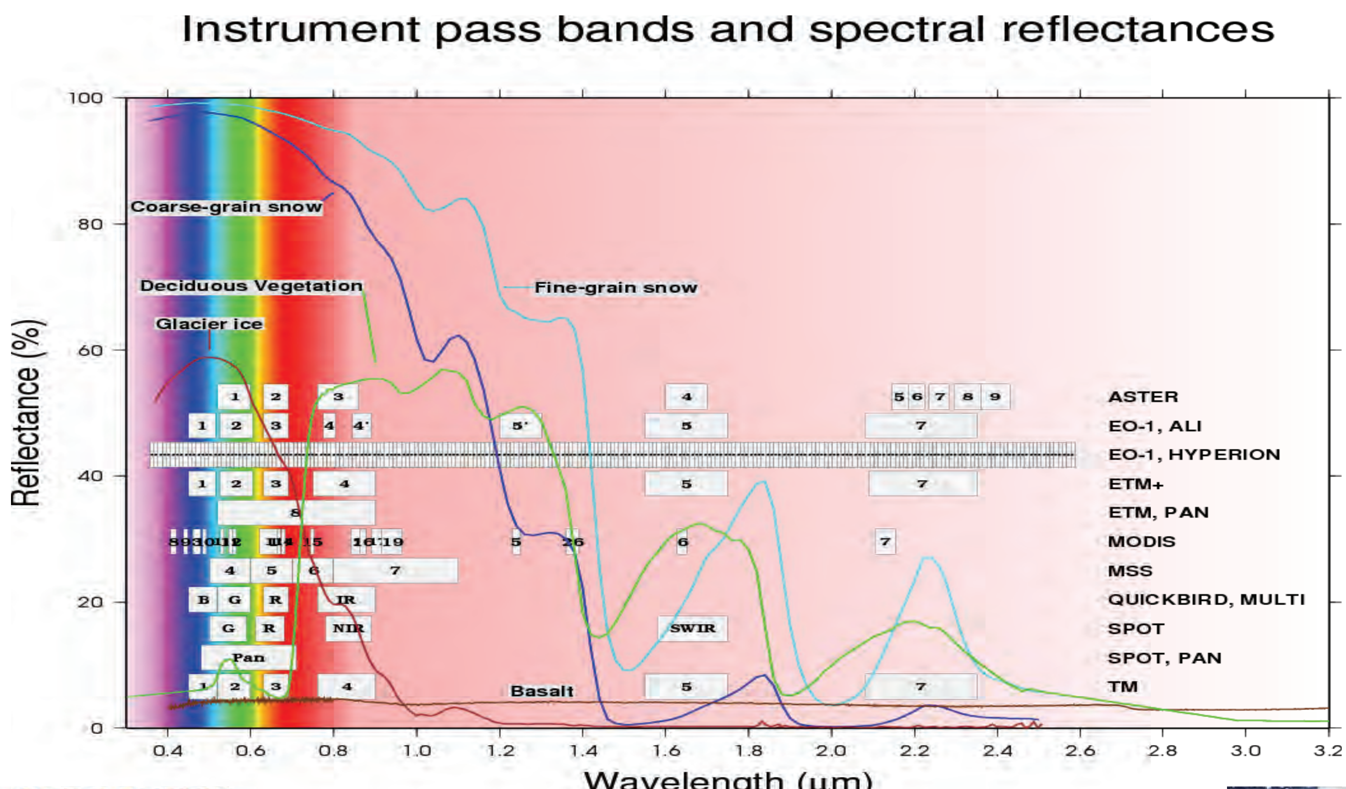

Grain size growth and albedo

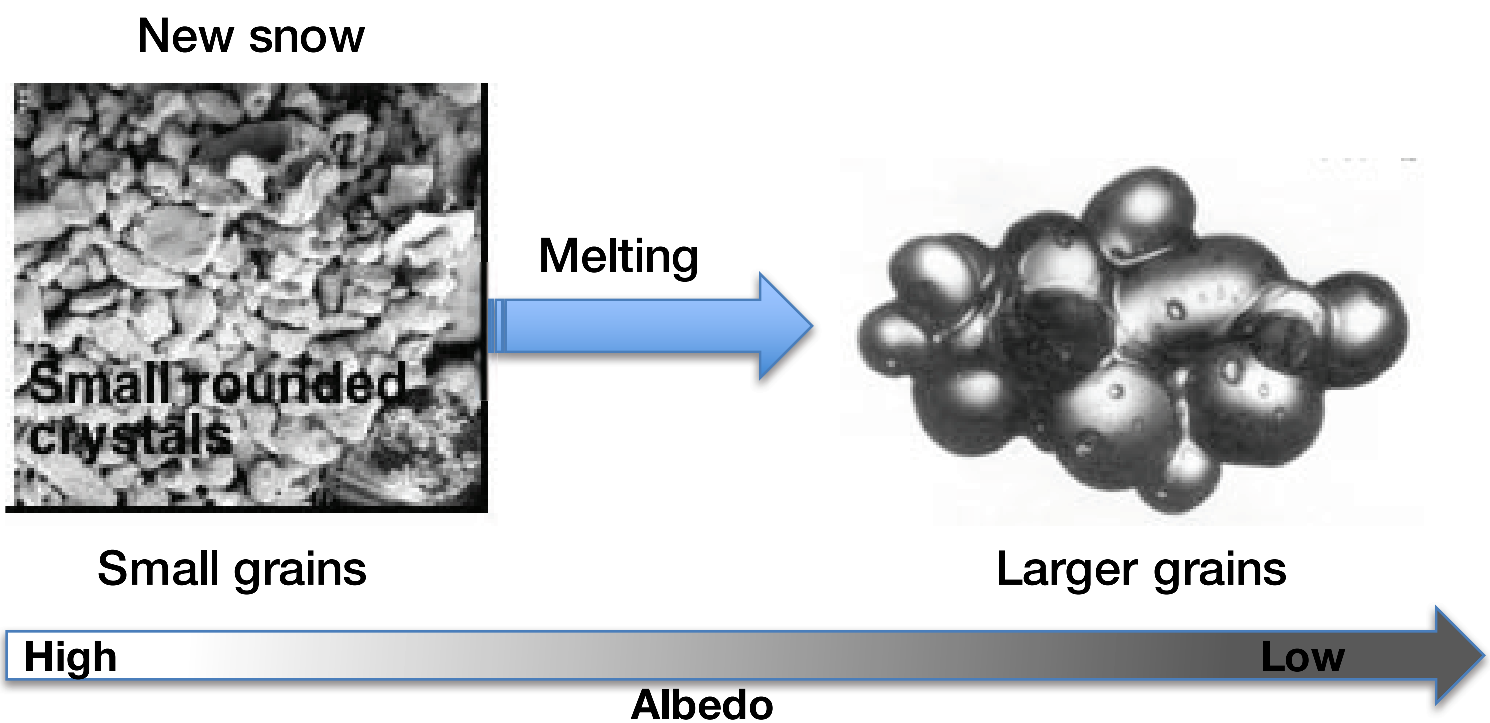

- Melting accelerates and promotes grain growth , in turn decreasing albedo in the near infrared

- This is INVISIBLE to our eyes but extremely powerful

Impurities (e.g., soot, dust) and albedo

Pure Snow

Melting

Dirty snow/ice

Albedo

High → **Low**

- As snow melts, impurities contained within the snowpack are deposited on the surface
- No evidence of direct impact of atmospheric deposition or forest fires on a seasonal scale
- Still, the impact of the 'cumulative' content of impurities is high

LAMONT-DOHERTY EARTH OBSERVATORY
THE EARTH INSTITUTE AT COLUMBIA UNIVERSITY

Grain size vs. impurities on albedo

Increasing grain size affects mostly NIR , with visible being weakly affected

Increasing the concentration of impurities affects mostly visible , with the impact on NIR being negligible

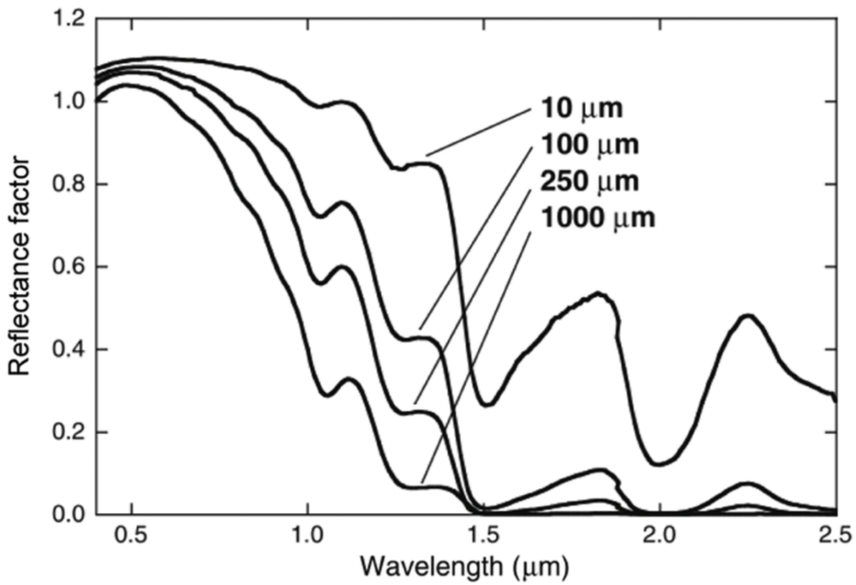

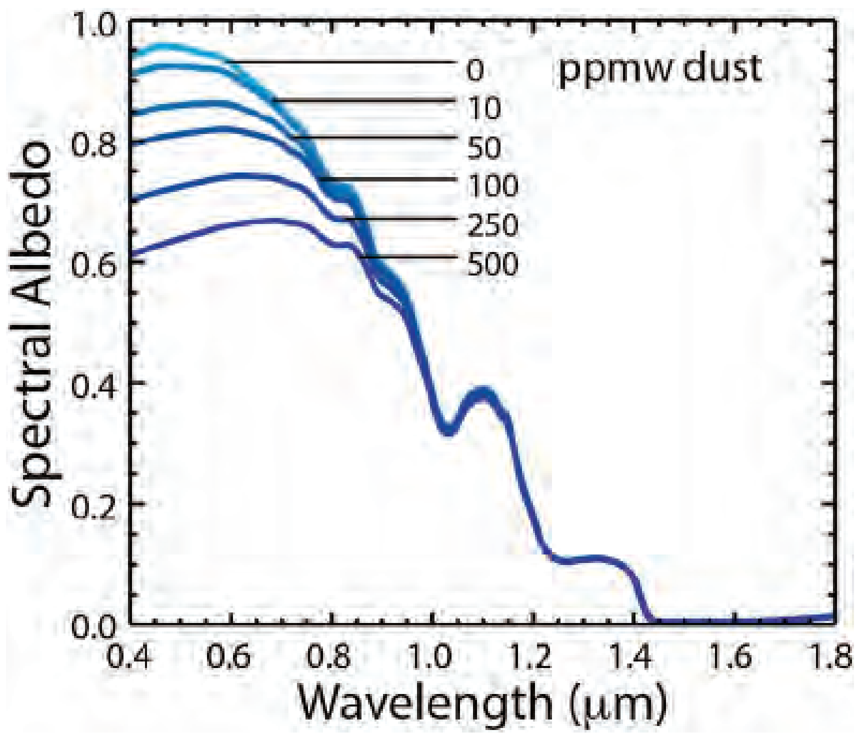

Examples of grain size estimates from MODIS

Snow grain size (mm) retrieved from MODIS TERRA data for the melting period of 2004 (April-August). Each image is obtained as a 3-day composite to cover gaps caused by clouds. The numbers give a Julian day (Reprinted from Lyapustin et al., 2009 with permission from Elsevier).

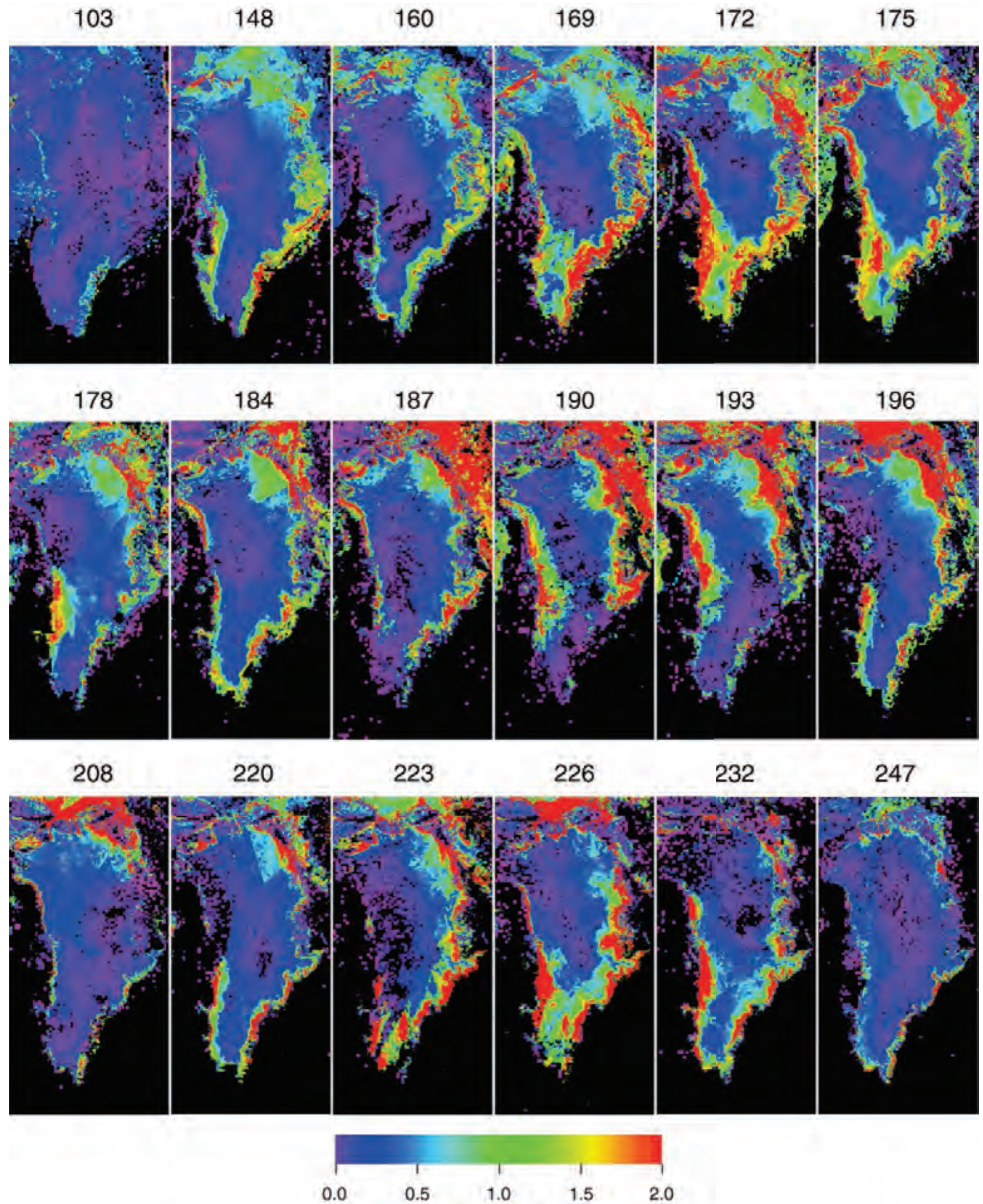

MODIS albedo anomaly maps and trends

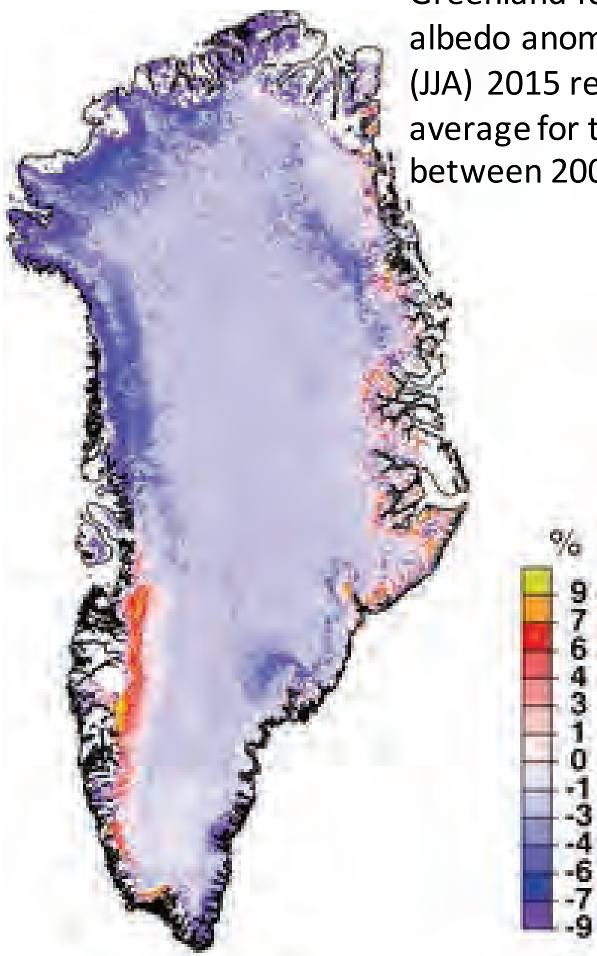

Greenland Ice Sheet surface albedo anomaly for summer (JJA) 2015 relative to the average for those months between 2000 and 2009.

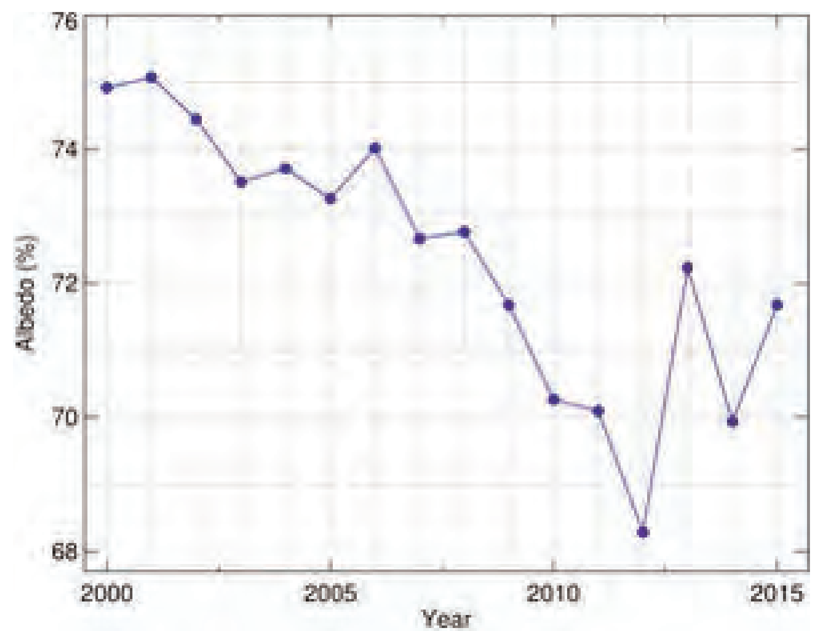

Average surface albedo of the entire ice sheet each summer (JJA) since 2000

Tedesco et al. Arctic report card 2015

MODIS albedo anomaly maps and trends

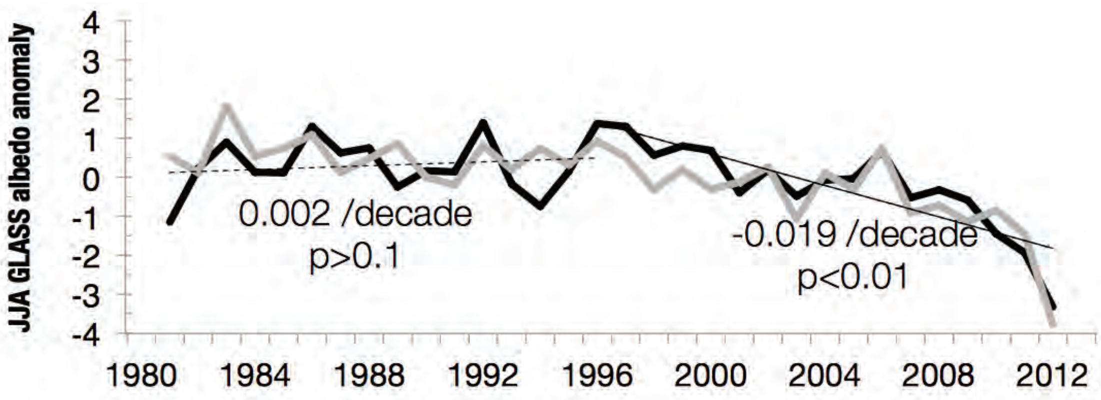

Mean summer standardized values plotted as time series for albedo from GLASS (black) → MODIS + AVHRR

Maps of JJA trends (per decade) from 1996 to 2012, when darkening began to occur, for (a) space-borne-estimated GLASS albedo

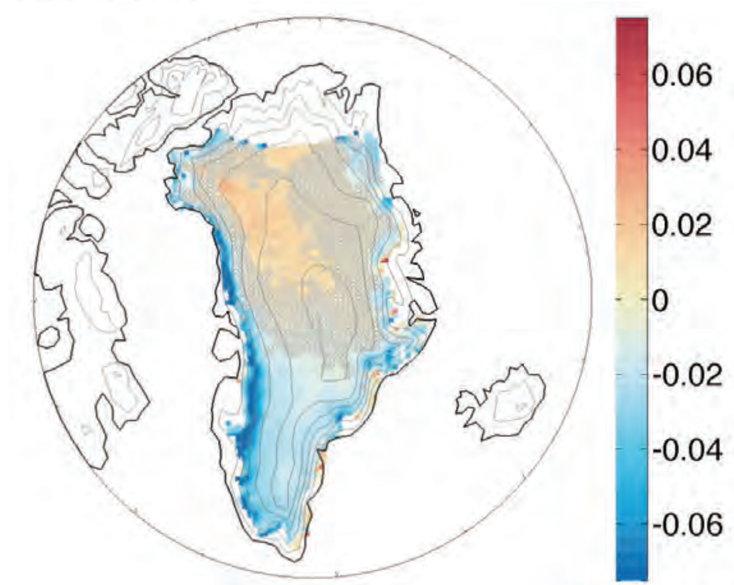

Tedesco et al. 2016

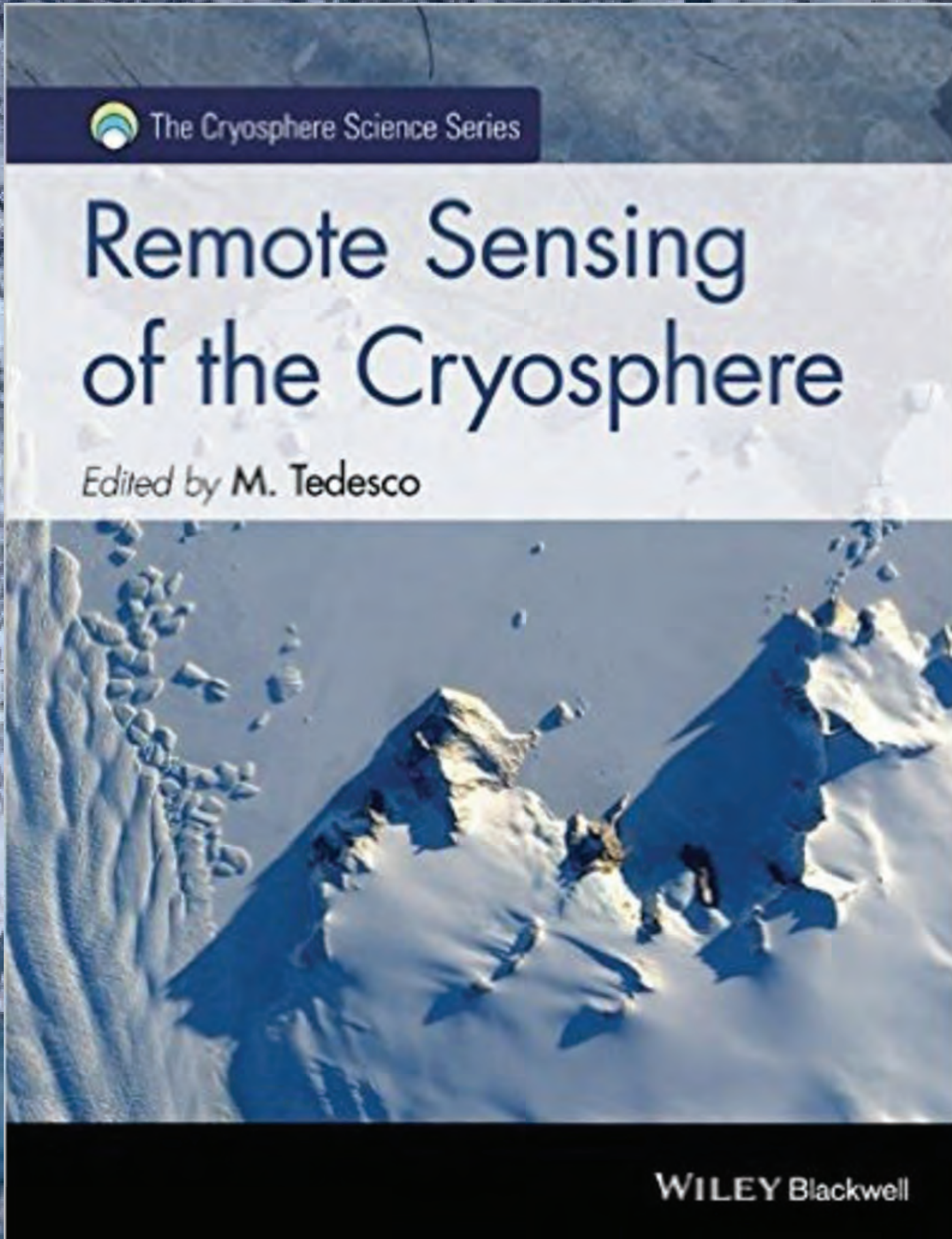
The Cryosphere Science Series
Remote Sensing of the Cryosphere
Edited by M. Tedesco
WILEY Blackwell

Questions ?